2018

Cognitive Load Reduces the Effects of Optic Flow on Gait and 2 Electrocortical Dynamics During Treadmill Walking 3

Brenda Malcolm
The Sheryl & Daniel R. Tishman Cognitive Neurophysiology Laboratory, Department of Pediatrics, Albert Einstein College of Medicine, New York, USA

John J. Foxe
Program in Cognitive Neuroscience, The Graduate Center of the City University of New York, New York, USA

John Butler
Technological University Dublin, john.s.butler@tudublin.ie

See next page for additional authors

Recommended Citation

Malcolm, B., Foxe, J. & Butler, J. (2018). Cognitive Load Reduces the Effects of Optic Flow on Gait and 2 Electrocortical Dynamics During Treadmill Walking 3. *Journal of Neurophysiology*, vol. 120, no. 5, pg. 2246-2259. doi: 10.1152/jn.00079.2018

Cognitive load reduces the effects of optic flow on gait and electrocortical dynamics during treadmill walking

Brenda R. **Malcolm** [1, 2], John J. **Foxe** [1, 2, 3, 4, 5, #], John S. **Butler** [1, 5, 6, 7], Sophie **Molholm** [1, 2, 3, 4] & Pierfilippo **De Sanctis** [1, 2, 8, #]

[1] *The Sheryl & Daniel R. Tishman Cognitive Neurophysiology Laboratory*
Children's Evaluation and Rehabilitation Center (CERC)
Department of Pediatrics
Albert Einstein College of Medicine
Bronx, New York 10461, USA

[2] *Program in Cognitive Neuroscience*
The Graduate Center of the City University of New York
New York, New York 10016, USA

[3] *The Del Monte Institute for Neuroscience*
Department of Neuroscience
University of Rochester School of Medicine and Dentistry
Rochester, New York 14642, USA

[4] *The Dominick P. Purpura Department of Neuroscience*
Rose F. Kennedy Intellectual and Developmental Disabilities Research Center
Albert Einstein College of Medicine
Bronx, New York 10461, USA

[5] *Trinity College Institute of Neuroscience*
Dublin, Ireland

[6] *Trinity College Dublin*
Centre for Bioengineering
Trinity Biomedical Sciences Institute
Dublin, Ireland

[7] *School of Mathematical Sciences*
Dublin Institute of Technology
Dublin, Ireland

[8] *The Saul R. Korey Department of Neurology*
Albert Einstein College of Medicine
Bronx, New York 10461, USA

Correspondence: john_foxe@urmc.rochester.edu and pierfilippo.sanctis@einstein.yu.edu

ABSTRACT

While navigating complex environments the brain must continuously adapt to both external demands such as fluctuating sensory inputs, as well as internal demands, such as engagement in a cognitively demanding task. Previous studies have demonstrated changes in behavior and gait with increased sensory and cognitive load, but the underlying cortical mechanisms remain unknown. Here, in a Mobile Brain/Body Imaging (MoBI) approach sixteen young adults walked on a treadmill with high density EEG and 3D motion capture tracked kinematics of the head and feet. Visual load was manipulated with the presentation of optic flow with and without mediolateral perturbations, and the effects of cognitive load were assessed by the performance of a Go/No-Go task on half of the blocks. During increased sensory load, participants walked with shorter and wider strides, which may indicate a more cautious pattern of gait. Interestingly, cognitive task engagement attenuated these effects of sensory load on gait. Using an Independent Component Analysis (ICA) and dipole-fitting approach, neuro-oscillatory activity was evaluated from source-localized cortical clusters. Significant modulations in spectral power in the theta (3-7Hz), alpha/mu (8-12Hz), beta (13-30Hz), and gamma (31-45Hz) frequency bands were observed over occipital, parietal and frontal source clusters, as a function of optic flow and task load. These findings provide insight into the neural correlates of gait adaptation, and may be particularly relevant to older adults who are less able to adjust to ongoing cognitive and sensory demands while walking.

Keywords: EEG, Mobile Brain/Body Imaging (MoBI), dual-task design, Independent Component Analysis (ICA), power spectral density

INTRODUCTION

Although we typically take walking for granted, the neural systems that regulate it perform many complex functions (Rossignol, Dubuc, & Gossard, 2006). Human locomotion involves the combination of descending pathways from the brainstem to the spinal cord (Duysens & Van de Crommert, 1998), the involvement of the cerebellum and basal ganglia to modulate posture and balance (Grillner, Wallen, Saitoh, Kozlov, & Robertson, 2008) and more recent evidence points to the direct involvement of cortical motor areas in the control of leg muscle activity (Artoni et al., 2017; T. H. Petersen, Willerslev-Olsen, Conway, & Nielsen, 2012). Moreover, when navigating new or unpredictable environments, cortical resources must be recruited to integrate numerous sources of sensory information including visual, vestibular, somatosensory and proprioceptive inputs (Jacobs & Horak, 2007; Varraine, Bonnard, & Pailhous, 2002), or to attend to cognitively demanding secondary tasks (De Sanctis, Butler, Malcolm, & Foxe, 2014). Behavioral studies have previously explored adaptations in gait in response to various manipulations in sensory and cognitive load, however much remains unknown about the cortical underpinnings of sensorimotor mechanisms during locomotion. Here, the aim was to assess the effects of both increased environmental (deployed with optic flow stimuli and visual perturbations) and cognitive load (either engaging in performing a cognitive task or not) on gait and neuro-oscillatory activity.

Vision provides a fundamental source of information for the control of goal-directed movements (Lappe, Bremmer, & van den Berg, 1999; W. H. Warren, Jr., Kay, Zosh, Duchon, & Sahuc, 2001). Optic flow, the visual motion we experience as a result of traveling through our environment (Lappe & Grigo, 1999) is a powerful signal that can be used to control the parameters of our movements. Prior studies have introduced perturbations and experimentally manipulated visual inputs to better understand how changes in the visual environment contribute to locomotion. For example, changing the speed of optic flow causes people to modulate their walking speed accordingly (Prokop, Schubert, & Berger, 1997) and the direction

of optic flow influences heading direction (Butler, Smith, Campos, & Bulthoff, 2010; Lappe et al., 1999; W. H. Warren & Hannon, 1988). Other studies have employed sinusoidally oscillating visual scenes and observed anisotropic changes in gait parameters, i.e. measures such as step width variability increased in magnitude in accordance with the degree and direction of visual perturbations (O'Connor & Kuo, 2009). Walking in a virtual reality (VR) environment matched to the speed of the treadmill, Hollman et al. (2006) found that young adults took shorter strides and wider steps, with increased variability in stride velocity and step width, compared to walking in a non-VR (visually static) environment, modulations they characterize as reflecting gait instability (Hollman, Brey, Robb, Bang, & Kaufman, 2006). Furthermore, likely due to the fact that humans are more unstable in the ML direction during locomotion (Bauby & Kuo 2000, Donelan 2004, Dean 2007, O'Connor & Kuo 2009) previous studies have noted an increased sensitivity to environmental perturbations in the mediolateral (ML) direction, opposed to those in the anterior-posterior (AP) direction. For example, ML oscillations introduced into a VR environment in the form of continuous but unpredictable (pseudo-random) perturbations resulted in participants taking shorter and wider steps with increased gait variability compared to the no-perturbation condition, but this effect was not observed with perturbations in the AP direction (McAndrew, Dingwell, & Wilken, 2010; McAndrew, Wilken, & Dingwell, 2011). These gait adaptations were interpreted as assuming a more cautious pattern of walking.

When navigating complex real-world environments, another challenge to walking behavior is the accommodation of an attentionally demanding secondary task, such as following directions or responding to a text message. Dual-task walking situations have been widely studied in various laboratory settings and with different populations, for reviews see (Al-Yahya et al., 2011; Woollacott & Shumway-Cook, 2002). Depending on the type and complexity of the secondary cognitive task, young adults have typically shown none or minimal costs in the maintenance of postural control (Woollacott & Shumway-Cook, 2002) and gait stability. However some reported changes in young adults' walking as a result of dual-tasking have

included reduced gait velocity (Hollman, Kovash, Kubik, & Linbo, 2007; Springer et al., 2006), reduced cadence and stride length, increased stride time and stride time variability (Al-Yahya et al., 2011) and decreased step width variability (Grabiner & Troy, 2005). These modulations have been interpreted as an adoption of a more conservative gait pattern, and may be explained in terms of a capacity sharing model of attentional trade-off (Pashler, 1994; Tombu & Jolicoeur, 2003) in which cortical resources recruited to maintain steady gait become taxed under conditions of increased cognitive load (O'Shea, Morris, & Iansek, 2002). Additional support for this model comes from findings in older adults who often exhibit greater costs in the form of gait instability, when engaged in a cognitive task (Yogev-Seligmann, Hausdorff, & Giladi, 2008). Finally, in nondemented older adults, declines in executive function were correlated with decreased walking speed (Ble et al., 2005) and increased gait variability (Springer et al., 2006). These studies provide indirect evidence of the presence of shared cortical resources for cognitively demanding tasks and the maintenance of gait stability.

Research using functional magnetic resonance imaging (fMRI) and motor imagery (Bakker et al., 2008), as well as functional near-infrared spectroscopy (fNIRS) (Harada, Miyai, Suzuki, & Kubota, 2009; Miyai et al., 2001) and transcranial magnetic stimulation (TMS) (N. T. Petersen et al., 2001; N. T. Petersen, Pyndt, & Nielsen, 2003), have provided additional evidence of cortical involvement in walking behavior. But due to the slow temporal resolution of hemodynamic measures, EEG, with its portability, relative low cost and excellent temporal resolution, has emerged as the method of choice to assess electrocortical functioning during active movements. When utilized in concert with body motion tracking this approach is referred to as Mobile Brain/Body Imaging (MoBI) (Gramann et al., 2011; Gramann, Jung, Ferris, Lin, & Makeig, 2014; Makeig, Gramann, Jung, Sejnowski, & Poizner, 2009). Recent MoBI studies from our group and others have established the viability (De Sanctis, Butler, Green, Snyder, & Foxe, 2012; Gramann, Gwin, Bigdely-Shamlo, Ferris, & Makeig, 2010) and long-term reliability (Malcolm et al., 2017) of recording event-related potentials (ERPs) reflecting cognitive

processes during treadmill and outdoor (De Vos, Gandras, & Debener, 2014) walking. Additional studies have employed the MoBI approach to measure differences in electrocortical activity and gait at varying levels of walking speed (De Sanctis et al., 2014; Kline, Poggensee, & Ferris, 2014), and have assessed age-related differences in behavior, gait and ERPs during dual-task walking (Malcolm, Foxe, Butler, & De Sanctis, 2015).

Other MoBI studies have provided evidence of suppression of oscillatory activity over motor cortex during walking (Cevallos et al., 2015; Presacco, Goodman, Forrester, & Contreras-Vidal, 2011) compared to standing, signifying increased activations during motion compared to at rest (Wagner et al., 2012), in agreement with prior research showing that efficient motor actions are associated with alpha (8-12Hz) and beta band (13-35Hz) rhythms, such as local field desynchronizations over sensorimotor and parietal cortex (Pfurtscheller, 2000; Pfurtscheller, Graimann, Huggins, Levine, & Schuh, 2003). Recording EEG activity during locomotion, researchers have also begun to investigate the cortical dynamics associated with different phases of the gait cycle during steady-state walking (Gwin, Gramann, Makeig, & Ferris, 2011; T. H. Petersen et al., 2012; Severens, Nienhuis, Desain, & Duysens, 2012), walking in synchrony with pacing tones (Wagner, Makeig, Gola, Neuper, & Muller-Putz, 2016) and when experiencing a loss of balance (Sipp, Gwin, Makeig, & Ferris, 2013). In an effort to explore the neurophysiological correlates of active vs. passive locomotion, Wagner et al. (2012) recorded EEG while participants walked in a Lokomat machine for robotic-assisted walking rehabilitation (Wagner et al., 2012). Spectral patterns over sensorimotor cortical areas revealed significant modulations in mu (8-12Hz), beta (18-21Hz) and gamma (25-40Hz) band frequencies, as well as activity that may represent the transition from stance to swing phase of the gait cycle.

A major issue in obtaining informative event-related cortical activity during walking is the presence of movement-related artifacts. While gait-specific activity has been identified in low EEG frequencies <10Hz (Castermans, Duvinage, Cheron, & Dutoit, 2014; Gwin, Gramann, Makeig, & Ferris, 2010; Kline, Huang, Snyder, & Ferris, 2015; Presacco, Forrester, & Contreras-

Vidal, 2012), several different groups have investigated different approaches that may be employed to successfully isolate and remove head movement and gait artifacts from cortical signals (Gwin et al., 2010; Kline et al., 2015; Nathan & Contreras-Vidal, 2015; Severens et al., 2012; K. L. Snyder, Kline, Huang, & Ferris, 2015). One approach involves using independent components analysis (ICA), already shown to be effective at separating eye and muscle-related noise from EEG signals obtained during seated tasks (Delorme, Sejnowski, & Makeig, 2007; Jung et al., 2000), combined with dipole fitting procedures that model independent components (ICs) as equivalent current dipoles (Oostenveld & Oostendorp, 2002), to accurately localize the resulting neural sources. Snyder et al. (2015) recently tested this tactic by recording EEG over a silicone swim cap, thus blocking all real electrophysiological activity, and demonstrated that ICA and dipole fitting procedures accurately isolated 99% of non-neural sources by location (outside of the brain) or by a lack of dipolar characteristics (K. L. Snyder et al., 2015).

Here, we employed a MoBI approach with young adult participants to evaluate the effects of environmental load, in the form of three different visual conditions (consistent optic flow, optic flow with visual perturbations and static) as well as cognitive load, on gait and electrocortical dynamics. Spatiotemporal measures of gait and variability in head movement were captured with kinematics recordings. Spectral power was obtained from high-density EEG using an ICA and dipole fitting procedure. Independent Component cluster models were then used to identify modulations in average spectral activity across participants as a result of optic flow and cognitive task load. We hypothesized that increased load during walking would lead to a more conservative and more variable pattern of gait. Furthermore, previous literature has reported increased cortical excitability exhibited in the form of power reductions, or desynchronization, in the alpha frequency band over occipital regions during visual processing (Pfurtscheller & Lopes da Silva, 1999), as well as in the mu and beta bands before and during movements (Pfurtscheller & Klimesch, 1991; Wagner et al., 2012). In line with these findings, we predicted that increased sensory load (optic flow vs. static) and cognitive load (processing

letters vs. not processing letters) would lead to a decrease in alpha power over occipital regions, and decreased mu and beta power over sensorimotor cortex. Finally, based on literature linking increased alpha power over parietal regions to attentional mechanisms used to suppress task-irrelevant information (Foxe & Snyder, 2011), we predicted that sensory load, particularly unreliable visual scene motion in the form of mediolateral perturbations, would result in increased alpha power over parietal cortex.

METHODS

Participants

Eighteen healthy young adults participated in the experiment. Data from two participants were excluded due to technical issues; therefore results reported here were derived from sixteen individuals (five females) with a mean age of 25.6 years (SD = 4.5 years). All individuals reported normal or corrected-to-normal vision and were free from any neurological, psychiatric or locomotor disorders, by self-report. Participants were recruited from the lab's existing subject pool and from flyers posted at the Albert Einstein College of Medicine. The Institutional Review Board of the Albert Einstein College of Medicine approved the experimental procedures and all participants provided their written informed consent. All procedures were compliant with the principles laid out in the Declaration of Helsinki for the responsible conduct of research.

Stimuli and procedure

While walking on the treadmill, participants were presented with a full-field visual display consisting of a star field (200 randomly placed white dots projected onto a black background). In the two dynamic optic flow conditions, the stars emanated outward from a central focus of expansion point, either moving steadily with no visual perturbations (NOP) or oscillating with continuous perturbations in the mediolateral direction (MLP). Optic flow was programmed from:

$$D(t) = A \times \sin(0.4 \times 2\pi t)$$

Where D(t) was the translation distance (m), A was the amplitude of displacement and *t* was time (sec). Sinusoidal perturbations in the ML direction were applied at amplitudes of 0 (NOP condition) or 0.12 m (MLP condition). The frequency selected (0.4 Hz) was within the range of those used in previous studies of human gait (McAndrew et al., 2010; O'Connor & Kuo, 2009). The star field moved in this manner throughout the duration of a three-minute walking block. A static condition was also employed in which the same number of stars were randomly presented across the visual field projection but did not move, i.e., no optic flow. Participants were instructed to keep their eyes fixed on a central fixation cross.

In addition to these three visual conditions, participants were presented with a Go/No-Go response inhibition task. Stimuli consisting of letters were shown in the center of the visual field, not interfering with the optic flow. During 'Task' blocks, participants were instructed to engage in the cognitive task by responding quickly and accurately to the frequently-occurring Go trials by clicking a wireless mouse button following the presentation of the letter 'O', while withholding responses during infrequent No-Go trials, designated by the presentation of the letter 'X.' The probability of Go and No-Go trials was 0.80 and 0.20, respectively. The duration of each letter was 400ms with a random stimulus-onset-asynchrony (SOA) ranging from 600-800ms. Response inhibition performance was assessed by a participant's percentage of Correct Rejection (CR) trials, defined as when a response was correctly withheld following a No-Go stimulus. In order to evaluate the effect of cognitive task load on gait and EEG spectral power, half of the experiment was performed as 'No-Task' blocks, in which the Go/No-Go stimuli were shown but participants were instructed not to respond to the task, or to cognitively engage in the task. Images were projected centrally (InFocus XS1 DLP, 1024 x 768 pixel) onto a black wall

approximately 1.5m in front of the participant. The stimulus display was programmed with Presentation software version 18.1 (Neurobehavioral Systems, Berkeley, CA).

With the two factors of visual condition (static, optic flow with no perturbation, optic flow with mediolateral perturbation) and cognitive task (task performance or no-task performance), this design resulted in a total of six different experimental conditions. Each participant performed three blocks of each condition, resulting in a total of 18 blocks, each lasting three minutes. All conditions were conducted in a pseudo-random order, counterbalanced across participants, and a practice block was performed before undertaking the main experiment. Several rest breaks were provided in between blocks. Participants self-selected their walking speed at the beginning of the experiment and maintained that speed throughout. Average walking speed was 3.9 km/hr (range: 3.2–4.5 km/hr). All subjects walked while wearing comfortable shoes and a safety harness. See Figure 1 for a representation of the recording set-up. No specific task prioritization instructions (i.e., walking versus cognitive task) were given, other than for participants to direct their gaze towards the central fixation cross (and presentation of task-relevant letters) during no-task as well as task blocks.

Insert Figure 1 Here

Kinematics recording

Three-dimensional kinematic data were collected at 100Hz using a 9-camera Optitrack infrared motion capture system and Arena v.1.5 acquisition software (Natural Point). Each participant wore 10 reflective markers: four were placed on the head (attached to the EEG cap, right and left sides, front and back), and three markers were placed on each foot. These were placed over the participants' shoes, on the calcanei, the second and the fifth distal metatarsals.

Electrophysiological recording

Continuous EEG was recorded with a 72-channel BioSemi ActiveTwo system (digitized at 512Hz; 0.05 to 100 Hz pass-band, 24 dB/octave). Stimuli from Presentation software were transmitted to BioSemi Actiview via a parallel cable. Time-synchronized acquisition of stimulus triggers, behavioral responses, EEG and rigid body motion tracking was conducted with Lab Streaming Layer software (Swartz Center for Computational Neuroscience, UCSD, available at: https://github.com/sccn/labstreaminglayer).

Data Analysis

All EEG and kinematic data analyses were performed using custom MATLAB scripts (MathWorks, Natick, MA) and EEGLAB (Delorme & Makeig, 2004).

Kinematics

Heel strikes were computed from the heel marker trajectory, using an automated peak-picking function (MATLAB custom scripts) and confirmed by manual inspection, to identify the point where the heel marker was at the most anterior point in the anterior-posterior direction (Dingwell, John, & Cusumano, 2010; Zeni, Richards, & Higginson, 2008). Individual strides were defined as consecutive heel strikes of the same foot. Responses to visual optic flow and cognitive task load on the gait cycle were assessed by three dependent measures. Stride time (ST) was defined as the time between consecutive heel strikes of the same foot, while Stride length (SL) was calculated as the sum of each pair of consecutive step lengths that made up each stride (Alton, Baldey, Caplan, & Morrissey, 1998; Dingwell & Cusumano, 2015). Step width (SW) was computed as the lateral distance between the two heel markers at the time of right heel strike (Kang & Dingwell, 2008; Kline et al., 2014; Owings & Grabiner, 2004). The means and standard deviations of each of these measures were calculated for each block of each condition, for each participant. Finally, the mean SD of the head markers in the mediolateral and

anterior-posterior directions was used as a measure of postural stability and overall variability in movement position on the treadmill. The SD was calculated for each block separately, and then averaged over conditions, then subjects.

EEG and power spectral density

EEG data were first high-pass filtered at 1Hz using a zero phase FIR filter (order 5632) (Winkler, Debener, Muller, & Tangermann, 2015). Then all blocks for each subject were concatenated into one dataset. Noisy channels were identified and removed by visual inspection and by automatic detection of channels with signals more than five times the standard deviation of the mean across all channels. The remaining channels were re-referenced to a common average reference. Continuous data were then subjected to a manual visual inspection resulting in the rejection of any sequences that contained large or non-stereotypical artifacts. An extended Independent Components Analysis (ICA) decomposition was performed on the remaining data using default training mode parameters (Makeig, Bell, Jung, & Sejnowski, 1996). ICA separates various generators of task-evoked cortical activity to help distinguish and separate from artifactual sources such as electrical noise, eye blinks, neck muscles and walking-related artifacts such as cable sway (Jung et al., 2000).

The resulting Independent Components (ICs) were then coregistered with a standard MNI (Montreal Neurological Institute) boundary element head model and fit with single equivalent current dipole models using the DIPFIT toolbox in EEGLAB (Delorme, Palmer, Onton, Oostenveld, & Makeig, 2012; Oostenveld & Oostendorp, 2002). Only ICs for which the estimated dipole model was located within the brain and explained > 85% of the variance of the IC scalp map were retained (Gwin et al., 2011). These were then examined and any that were clearly artifactual were rejected; these could have included activity originating from eye blinks, bad electrodes and muscle noise. Rejection criteria were based on topography, spectra, component activation time course, and dipole location (Jung et al., 2000). Following this

procedure there were an average of 10 brain related ICs per participant (ranging from 6 to 16 ICs) for use in further analyses. Presumably, these ICs reflect activity generated in cortical sources close to the location of their equivalent dipole model (Akalin Acar & Makeig, 2013). Remaining ICs were then clustered across participants with EEGLAB clustering routines using the parameters of 3-D dipole location, scalp topography and power spectra (3-45Hz) (Onton & Makeig, 2006). Using principal components analysis, these feature vectors were reduced to 10 principal components and clustered using a k-means algorithm implemented in EEGLAB. *K*-means is a well-known clustering algorithm that requires no prior information about the associations of data points with clusters. ICs that were further than three standard deviations from any of the resulting cluster centers were identified as outliers. Finally, only clusters that included ICs from at least half of the participants were retained, resulting in the eight clusters reported below.

For the spectral analysis, we chose to look at the neural oscillatory pattern resulting from component activations, in comparison to the data from separate channels, since independent components may help to explain the activity underlying a specific cognitive function. whereas channel activations are the result of summed potentials volume-conducted from different parts of the brain (Onton, Westerfield, Townsend, & Makeig, 2006). Even though EEG does not have the spatial resolution of fMRI, this technique has been shown to provide a spatial resolution of around a few centimeters (Mullen, Acar, Worrell, & Makeig, 2011). Power spectral density (PSD) was computed using Welch's method, separately for each IC and for each of the six experimental conditions. Periodograms were obtained in windows of 512 samples (1 sec), an fft length of 1024, with 50% overlap, and windowed with a Hamming window of the same length as the segment. Similar parameters were used to calculate spectra for ICs in a previous MoBI study (K. L. Snyder et al., 2015). The resulting periodograms were averaged over the ICs in each cluster to produce an estimation of the absolute PSD for four frequency bands of interest: theta (3-7Hz), alpha (8-12Hz), beta (13-30Hz) and gamma (31-45Hz).

Statistical analyses

Cognitive task performance was analyzed with a one-way repeated-measure ANOVA, with the factor of visual load (static, no perturbation optic flow and ML optic flow). Gait and posture data were analyzed with 2 (Task Load) x 3 (Visual Load) repeated measures ANOVAs. Because walking speed has a direct relationship with stride length and stride time (Dingwell et al., 2010; Kang & Dingwell, 2008) walking speed was included as a covariate in the analysis of these gait parameters. The covariate was mean-centered, i.e., deviations from the mean speed were used instead of the raw values, to avoid interfering with the test of the main effects (Delaney & Maxwell, 1981). For the analysis of power spectral density (PSD), separate two-factor (task load, visual condition) repeated-measures ANOVAs were performed for each IC cluster and frequency band of interest. Greenhouse-Geisser corrections were applied when appropriate, but original degrees of freedom have been reported. All statistical analyses were performed using IBM SPSS (v. 24).

RESULTS

Cognitive Task Performance

Figure 2 shows the percentage of Correct Rejections (CRs) for each visual condition (static, no perturbation optic flow and optic flow with ML perturbations). No differences were found for response inhibition performance as a function of the visual condition employed, $F_{2, 30} = 0.27$, $p = .76$, indicating that participants were able to perform the Go/No-Go task equally well regardless of the dynamic state of the star field.

Insert Figure 2 Here

Gait and Posture

Average and mean SD of stride time, stride length and step width for all six conditions are presented in Figure 3.

Stride Time: For the parameter of average stride time, there was a main effect of task load, $F_{1, 14} = 8.51$, $p = .01$, and an interaction between task load and visual condition, $F_{2, 28} = 3.99$, $p = .03$. Follow-up paired comparisons showed that, averaged over all visual conditions, participants took significantly faster strides when engaged in the task (Mean = 1179ms, SD = 75) compared to the no-task blocks (Mean = 1189ms, SD = 78), $t_{15} = 3.02$, $p = .009$. Furthermore, for the no-task conditions, participants exhibited increasingly faster strides with increasing levels of visual load. The slowest strides were observed for the static no-task condition, closely followed by the no perturbation optic flow condition. On the other hand, during the task blocks, there was minimal difference in average stride time according to visual stimuli. Averaging across task conditions revealed significantly longer strides for the no-perturbation optic flow condition in comparison to the presentation of ML perturbations ($p = .02$). For the measure of average stride time variability, no significant effects were found.

Stride Length: There was a main effect of visual condition on average stride length, $F_{2, 28} = 3.59$, $p = .04$, as well as a significant effect of task load, $F_{1, 14} = 11.85$, $p = .004$, and an interaction was observed between these two factors, $F_{2, 28} = 5.43$, $p = .01$. In line with the findings outlined above for Stride Time, participants took significantly shorter strides when engaged in the task (Mean = 1423mm, SD = 115) compared to not performing the task (Mean = 1438mm, SD = 122), $t_{15} = 3.50$, $p = .003$. The effect of visual condition on average stride length exhibited the greatest difference between the static star field condition in which participants took overall longer strides, compared to the ML visual perturbations ($p = .04$). This effect also appeared to be most prominent for the no-task blocks, as stride length progressively decreased

with the dynamic optic flow and even more so as perturbations were applied to the star field. For stride length variability no effects reached the level of significance, though interestingly, strides tended to be more variable when participants observed the dynamic optic flow and were not engaged in the cognitive task.

Step Width: There was a significant effect of the visual condition on average step width, $F_{2, 28}$ = 7.14, p = .003, reflecting the fact that compared to the static visual condition, participants walked with wider steps during the no perturbation optic flow blocks (p = .002) as well as with ML perturbations (p = .02), regardless of whether they performed the cognitive task. Average step width variability exhibited a robust effect of task load, $F_{1, 14}$ = 11.77, p = .004, with more variable step widths across all visual conditions when not performing the cognitive task (Mean = 16.2mm, SD = 4.8), compared to during task blocks (Mean = 14.5mm, SD = 3.7).

Insert Figure 3 Here

Mean SD of head position: Figure 4 shows the mean SD of head position in the mediolateral (ML) direction (left) and anterior-posterior (AP) direction (right). For head position variability in the ML direction, there was a main effect of task load, $F_{1, 15}$ = 8.56, p = .01, indicating decreased variability in head position in the lateral direction when performing the cognitive task (Mean = 26.7mm, SD = 9.2) in contrast to walking without engaging in the task (Mean = 29.6mm, SD = 10.8).

For the average variability in head position in the AP direction, there was also a main effect of cognitive task load, $F_{1, 15}$ = 10.12, p = .006, as well as an interaction between cognitive load and visual condition, $F_{2, 30}$ = 7.33, p = .003. This effect was indicative of increased variability on the no-task blocks (Mean = 44.8mm, SD = 19.2) compared to performing the task

(Mean = 33.5mm, SD = 18.0), and while the different task blocks were shown to maintain a similar level of variability, the no-task conditions showed a decrease in variability from the static visual condition, to the no perturbation optic flow, and then even more so with the introduction of ML perturbations.

Insert Figure 4 Here

Power spectral density

Table 1 lists the specifics (number of ICs and subjects included in each cluster and the approximate anatomical location (Brodmann area and Tailarach coordinates) of cluster centroids) of the eight clusters that were localized to cortical areas and composed of ICs from at least half of the participants. Figure 5 shows the clusters of electrocortical sources localized to occipital, parietal and frontal cortical areas.

Insert Table 1 Here

Insert Figure 5 Here

Three clusters were located over occipital cortex. Scalp topography, dipole location (blue dots indicate the location of each IC, red dots represent the cluster centroid) and average power spectral density (PSD) for these clusters are presented in Figure 6. For the cluster located over medial occipital cortex, no significant modulations were found in the PSD of any frequency

bands according to task load or visual condition. In contrast, for the right occipital cluster, robust differences in spectral power attributable to the presentation of the three different visual conditions were found in theta, $F_{2, 22} = 8.94$, $p = .008$ and alpha, $F_{2, 22} = 21.50$, $p < .001$, frequencies, with a smaller effect observed in the beta range, $F_{2, 22} = 4.18$, $p = .05$. The same pattern emerged for the lower frequencies (theta and alpha) in that there was on average higher spectral power for the static conditions compared to both dynamic optic flow conditions (*p's* < .05), but no difference between the two optic flow conditions (*p's* > .50). For the beta range, increased power was observed during the static conditions compared to the no perturbation optic flow ($p = .006$), but no significant differences were found between the static and ML optic flow or between the two dynamic conditions (*p's* > .10). Furthermore, there was a strong effect of task load on alpha spectral power, $F_{1, 11} = 14.15$, $p = .003$, with higher power over all three no-task conditions compared to when participants performed the cognitive task. Finally, a significant interaction between task load and visual condition was found for gamma band power, $F_{2, 22} = 4.96$, $p = .02$, indicating that while spectral power remained relatively consistent across the visual conditions when participants engaged in the cognitive task, when they did not perform the task gamma power remained high for the static visual condition but decreased greatly during the no perturbation optic flow blocks, and decreased to a lesser extent with ML perturbations in optic flow.

For the IC cluster located in left occipital cortex, modulations in spectral power were only observed in the alpha frequency range. There was a robust effect of visual condition, $F_{2, 26} = 10.76$, $p = .004$, with higher alpha power observed for the static visual condition compared to both dynamic conditions (*p's* = .005) but no difference apparent between the two dynamic conditions ($p = .88$). There was also a trend towards higher alpha power on no-task blocks, $F_{1, 13} = 4.52$, $p = .053$, compared to blocks when participants engaged in the cognitive task.

Insert Figure 6 Here

Figure 7 shows scalp topography, dipole location and power spectra for one cluster over left temporal cortex and two clusters located over right parietal cortex. For the cluster localized to the left superior temporal gyrus, the different visual conditions had a significant effect on both theta band ($F_{2, 22} = 7.00$, $p = .02$) and alpha band ($F_{2, 22} = 9.65$, $p = .001$) spectral power. Both frequency bands showed significantly greater power during the static visual blocks compared to both dynamic optic flow conditions (*p's* < .05), with no differences between the two dynamic conditions (*p's* > .05). Additionally, no differences were apparent at higher frequencies. For the cluster localized to the right inferior parietal lobule, the only significant difference in spectral power was observed for the factor of visual condition in the alpha frequency range, $F_{2, 18} = 5.94$, $p = .01$. Again, regardless of task load, there was higher alpha power during the static star field blocks in comparison to both of the optic flow conditions (*p's* < .02), but there was no difference in power between the two dynamic star field displays ($p = .66$).

Significant modulations in spectral power as a result of visual condition were observed in the cluster of ICs located over medial parietal cortex, localized to the precuneus. This effect occurred across all frequency bands of interest: theta ($F_{2, 28} = 20.09$, $p < .001$), alpha ($F_{2, 28} = 15.63$, $p = .001$), beta ($F_{2, 28} = 10.33$, $p < .001$), and gamma ($F_{2, 28} = 3.66$, $p = .04$). For frequencies in the theta, alpha and beta bands, significantly greater power was observed for the static condition compared to both the no perturbation optic flow (*p's* < .01), and the ML perturbation condition (*p's* < .01), but there was no difference between the two optic flow conditions (*p's* > .05). In the gamma range only a significant difference between static and ML perturbations was observed ($p = .05$) but there was no difference between static and no perturbation ($p = .22$) or between the two optic flow conditions ($p = .24$). For the alpha and beta frequency bands, differences were also observed in spectral power linked to cognitive task

engagement: alpha ($F_{1, 14}$ = 21.07, p < .001), beta ($F_{1, 14}$ = 13.16, p = .003). For both, overall higher power was found for the no-task blocks compared to when participants performed the task. Finally, for frequencies in the alpha range there was an interaction between task load and visual condition, $F_{2, 28}$ = 5.94, p = .007, indicating that while either performing the cognitive task or not, there was a desynchronization in alpha power between the static visual condition to the no-perturbation optic flow condition, whereas a different result was observed with the introduction of ML perturbations. When performing the task, average power continued to decrease when perturbations were introduced into the optic flow, but when not engaged in the task, alpha power actually increased with the ML perturbations.

Insert Figure 7 Here

The final two clusters located over frontal cortical areas including the supplementary motor area and the anterior cingulate are depicted in Figure 8. For the cluster located over supplementary motor area, significant changes in spectral power were found in the theta range linked to task performance, $F_{1, 22}$ = 9.41, p = .006, representing the effect that average spectral power was higher when subjects performed the cognitive task compared to when they did not. Significant effects of the visual condition on spectral power were observed in the theta ($F_{2, 44}$ = 5.01, p = .02), alpha ($F_{2, 44}$ = 29.52, p < .001) and beta ($F_{2, 44}$ = 17.20, p < .001) bands. For alpha and beta this was reflected in the fact that higher spectral power was observed for the static condition compared to both no perturbations (*p's* < .001) and ML perturbations (*p's* < .001), whereas no difference occurred between the two dynamic conditions (*p's* > .05). For the theta range, spectral power during the ML perturbation conditions were significantly lower compared to presentation of the static star field (p = .006), as well as the no perturbation optic flow (p =

.04), while there was no difference between the static and no perturbation conditions (p = .19). Additionally, for frequencies in the alpha range, there was a significant interaction between task load and visual condition, $F_{2, 44}$ = 5.77, p = .01, indicating that the average spectral power remained approximately the same between task conditions for both the static and no perturbation star field displays, however with ML visual perturbations spectral power increased during no-task blocks but decreased with task engagement.

Lastly, for the IC cluster located to anterior cingulate cortex, significant changes in spectral power were observed only in lower frequencies. The visual conditions significantly affected spectral power in both the theta ($F_{2, 28}$ = 10.16, p < .001) and alpha ($F_{2, 28}$ = 10.13, p < .001) frequency ranges. This effect was indicative of greater power for the static visual condition compared to both the no perturbation optic flow (p's < .005) and the ML perturbation optic flow (p's < .005), but no difference was apparent between the two dynamic conditions (p's > .10). Additionally, in the theta range, spectral power significantly increased during performance of the cognitive task in comparison to no-task blocks, across all three visual conditions, $F_{1, 14}$ = 11.61, p = .004.

Insert Figure 8 Here

DISCUSSION

Effects of optic flow and cognitive load on gait

The objective of the current experiment was to examine changes in gait and cortical network activity in response to the presence of optic flow stimuli, as well as the engagement or lack of engagement in a cognitive task. During two dynamic visual conditions a pattern of optic

flow created by the movement of a star field radiating outwards generated a sense of forward movement. The optic flow either moved steadily (no perturbations) or oscillated with continuous mediolateral (ML) perturbations. Sensory load, presented here in the form of optic flow, did not result in decrements in task performance, i.e., there were no costs in the behavioral domain as a result of the different visual conditions. Conversely, both sensory and cognitive load had significant effects in the motor domain. Participants took shorter strides as cognitive and sensory load increased. Average step width also increased with visual load, with wider steps during both optic flow conditions compared to the static star field. However, the interactions observed between cognitive and sensory load for the measures of stride time/length and head position in the AP direction reveal that optic flow modulates gait more so when participants are disengaged from the cognitive task. For example, participants made faster and shorter strides during both optic flow conditions compared to the static condition, when they were not engaged in the task. Also, during no-task blocks, average head position variability in the anterior-posterior (AP) direction decreased as the amount of visual load increased, i.e., in the presence of optic flow and even more so with the introduction of ML perturbations. These findings likely indicate the engagement of a more conservative pattern of gait with increased load: shorter and wider steps, and the maintenance of a more consistent position along the length of the treadmill. This may be indicative of increased allocation of sensorimotor resources in order to accommodate potentially destabilizing sensory load.

The primary effect of increased cognitive load on gait appeared to be a reduction in walking variability. When performing the inhibitory control task, participants exhibited decreased variability in step width and head position in both directions. These findings suggest that cognitive task engagement actually led to a more consistent pattern of motor behavior. Participants adopted a more stereotyped manner of walking, with less stride-to-stride fluctuations when attention was bound to the Go/No-Go task. Prior dual-task walking (DTW) findings seem to go along with these results, as Grabiner & Troy (2005) also observed

593 decreased step width variability and more conservative gait under cognitive load (Grabiner &
594 Troy, 2005). Additionally, Lovden et al. (2008) observed that when young adults performed a
595 moderately difficult cognitive task, gait variability decreased (Lovden, Schaefer, Pohlmeyer, &
596 Lindenberger, 2008). They contend that an external focus of attention is beneficial to motor
597 performance, and that there will be no cross-domain competition, resulting in costs, as long as
598 cognitive load remains moderate (Lovden et al., 2008).

599 Interestingly, when the ML perturbations were applied to the optic flow, participants often
600 did not exhibit increased movement in that direction, in relation to the no-perturbation optic flow.
601 This was somewhat surprising considering that other studies have observed effects such as
602 changes in posture and increased variability in gait and dynamic stability (McAndrew et al.,
603 2011) in response to ML visual perturbations. One possible reason that this may have occurred
604 is that participants in this study walked in a safety harness and wore an EEG cap, with
605 electrodes tethered to an overhead platform. Another explanation for the relative lack of
606 modulation in body position in the ML direction is that participants may have become
607 accustomed to the perturbations over time and were able to 'entrain' their walking behavior to
608 accommodate them. Because the ML visual oscillations were constant for the duration of each
609 three-minute block, in contrast to some studies that have employed pseudo-random
610 perturbations (McAndrew et al., 2010; McAndrew et al., 2011), participants here may have
611 unconsciously come to predict the effect that oscillations may have had on body position and
612 adjusted their gait accordingly. For example, Brady et al (2009) applied continuous ML
613 perturbations to the treadmill surface and observed that within five minutes people showed
614 adaptation in the form of entrainment and began to time their steps to occur in line with the
615 phase of oscillation applied (Brady, Peters, & Bloomberg, 2009). Also, in a very recent study,
616 young adults quickly adapted to continuous mediolateral optic flow perturbations by taking
617 shorter, wider and more variable steps, until after approximately three minutes step length and
618 width returned to normal (unperturbed) levels, while variability did not (Thompson & Franz,

2017). The authors attribute these results to visuomotor adaptation processes – the return of step length and width to normal levels as visual perturbations continued likely reflects a deprioritization of visual inputs while presumably other inputs, such as vestibular and proprioceptive modalities were up-regulated. On the other hand, they point to the sustained increase in variability as indicative of a necessary, reactive step-to-step balance control strategy.

There were a few gait parameters in which a significant difference was found between the two optic flow conditions (e.g., shorter strides and less variability in AP head position with added ML perturbations). These findings are consistent with other studies that have employed constant, sinusoidal oscillations and have still observed changes in measures such as step width (O'Connor & Kuo, 2009) and stride length variability. It is possible that when people come to predict the environmental perturbations, they will exhibit consistent changes in gait to better accommodate them. For example, that participants walked with faster and shorter strides and increased step width could be interpreted as a more cautious gait approach in response to sensory load. Furthermore, walking on a treadmill requires the strict regulation of both walking speed and position, but Dingwell (2015) showed that young adults regulated stride-to-stride fluctuations in walking by prioritizing speed maintenance, not their position in the anterior-posterior direction, therefore letting themselves drift to the front and back of the treadmill before correcting (Dingwell & Cusumano, 2015). This notion may explain the current finding of increased influence of visual flow on head position variability only in the AP direction, not the ML direction. When walking without additional cognitive load, participants may have allowed themselves to drift forwards and backwards on the treadmill, especially during the static no-task condition (perhaps the least attentionally demanding).

Modulations in power spectral density

Following an Independent Components Analysis (ICA) and dipole-fitting procedure, neuro-oscillatory activity was evaluated from eight source-localized clusters of Independent Components (ICs). To identify modulation in the power content across different frequencies as a function of visual load and cognitive task engagement, power spectral density (PSD) was calculated for each condition in each IC, and then averaged over all ICs in each cluster. These results provide new information about the frequency-related effects of optic flow stimulation and task load on brain activity during locomotion. The locations of the IC clusters reported here were similar to locations cited in other mobile EEG studies (Gwin et al., 2011; Kline, Huang, Snyder, & Ferris, 2016; Sipp et al., 2013; Wagner et al., 2012): three clusters were located over occipital cortical areas, one cluster localized to the left superior temporal gyrus, right inferior parietal lobule, the precuneus in the parietal lobe, and two frontal clusters over supplementary motor area and anterior cingulate cortex. Results indicate a widely distributed cortical network exhibiting task-specific fluctuations in spectral power.

Occipital Region

Other than the IC cluster over medial occipital cortex where no significant modulations were observed, all other clusters exhibited significant changes in the spectral power of lower frequencies (theta and alpha) linked to visual presentation and optic flow. For the right occipital cluster, average spectral power was reduced in the theta, alpha and beta ranges, with increased sensory load. In the left occipital cluster, this effect was also seen, but only in the alpha range. Additionally, decreased alpha power was also observed in the right occipital cluster as participants processed the Go/No-Go task letters; with a trend towards this effect in the left occipital cluster as well. Alpha band oscillations have long been shown to play an important role in directing attention, for a review see (Foxe & Snyder, 2011). Desynchronization in the alpha band over occipital regions is assumed to reflect cortical excitation related to various stages of stimulus processing (Pfurtscheller, Stancak, & Neuper, 1996), thus the reduction in alpha power

669 when presented with increased visual demands in the form of optic flow. Furthermore, EEG
670 studies of parieto-occipital alpha band activity have revealed a more sophisticated role as a
671 mechanism involved in selectively attending to relevant information in the environment (Foxe,
672 Simpson, & Ahlfors, 1998; Foxe & Snyder, 2011; Kelly, Lalor, Reilly, & Foxe, 2006; A. C. Snyder
673 & Foxe, 2010; Worden, Foxe, Wang, & Simpson, 2000). Presumably this paradigm required
674 participants to selectively disengage from processing the distracting optic flow information when
675 they were performing the task, reflected as synchronization in alpha power over cortical regions
676 dedicated to optic flow processing. Subsequently, during the blocks in which they saw the
677 Go/No-Go letters but were instructed to not engage cognitively, an effortful, top-down
678 recruitment strategy would likely be employed in order to ignore the letters, i.e., synchronization
679 in alpha to inhibit processing, but at the same time suppress any potentially destabilizing
680 information from the dynamic star field. Gait results indicate the adoption of a progressively
681 more conservative manner of walking with increased visual input but no task engagement.
682 Consequently, it seems that even though the optic flow lent no meaningful information to
683 walking behavior, on some level participants did pay attention to and process this information.
684 Thus, these findings may indicate a flexible deployment of enhanced alpha band activity to
685 selectively suppress to-be-ignored aspects of this complex environment (Dockree, Kelly, Foxe,
686 Reilly, & Robertson, 2007; Foxe & Snyder, 2011; Worden et al., 2000). This pattern of results is
687 consistent with alpha desynchronization not simply due to visual stimulation but being
688 specifically task driven (Kelly et al., 2006; Klimesch, 2012), a theory that goes along with the
689 current finding of a greater desynchronization in alpha power when individuals also engaged in
690 the task.

691 There was also an interaction between cognitive and sensory load in the gamma range
692 (31-45Hz) in the right occipital cluster. Here, gamma power increased while participants were
693 engaged in the Go/No-Go task, then decreased as they disengaged during no-task conditions,
694 though only while exposed to optical flow. Sustained attention requires ongoing activation of

task-relevant regions and evidence links gamma in sensory cortices as a mechanism to enhance processing of task-relevant sensory inputs (Clayton, Yeung, & Cohen Kadosh, 2015). Previous studies have also reported enhancement of gamma band activity during visuospatial attention tasks (Siegel, Donner, Oostenveld, Fries, & Engel, 2007) and gamma power has been associated with task complexity (Fitzgibbon, Pope, Mackenzie, Clark, & Willoughby, 2004). However, if sustained gamma power in this region is indeed related to sustained task engagement, it is an open question as to why the static no-task condition maintained a higher average spectral power in relation to the other no-task conditions.

Left Superior Temporal Gyrus

A main effect of visual condition was observed for theta and alpha activity in this region, with reductions in spectral power associated with increased optical flow input. Animal studies have shown that this area is involved in processing optic flow and visual motion information generated from environmental stimuli (Duffy & Wurtz, 1991). Therefore the current findings may indicate increased activation in this region when presented with more computationally demanding visual environments.

Parietal Region

The IC cluster localized to the right inferior parietal lobule showed a significant decrease in alpha spectral power for both dynamic flow conditions compared to the static visual condition. The precuneus cluster exhibited a similar pattern with decreased spectral power in theta, alpha and beta for optic flow relative to static, while gamma power was higher for the static condition relative only to visual ML perturbations. Thus, if we are to assume that participants invest more resources to counteract unreliable proprioceptive information (generated by ML visual perturbations), evidenced by their engagement in a more conservative pattern of gait, higher

gamma power during the static condition may be acting to increase reliance on proprioceptive information via enhanced sensory processing (Clayton et al., 2015).

The precuneus also showed modulations in spectral power as a result of cognitive task load, with activity in both alpha and beta bands ramping up during no-task blocks, possibly as a mechanism to inhibit and down-regulate visual load (Banerjee, Snyder, Molholm, & Foxe, 2011; Foxe et al., 1998; Foxe & Snyder, 2011). Furthermore, an interaction between visual and cognitive load within the alpha-band reveals that power decreases with visual load as participants are engaged in the cognitive task, but increases as participants disengage from the task, particularly while exposed to mediolateral perturbations. Considering precuneus connections with sensorimotor regions (Cavanna & Trimble, 2006), the latter finding might indicate an alpha-band mediated gating/suppression mechanism of unreliable information to sensorimotor regions. Interestingly, the IC clustering approach produced two parietal clusters, sensitive to attentional demands resulting from cognitive task engagement and the radiating star field, that were both localized to the right hemisphere. This finding fits nicely with several reports in the literature. The precuneus has been linked to the processing of scenes, with previous imaging studies reporting middle parietal cortex to be involved in visuospatial processing (Harris et al., 2000), and specifically the right hemisphere to be more spatially oriented to the surrounding environment (Joseph, 1988). Topographic mapping of high-density EEG recorded in a line-bisection task revealed a right hemisphere dominant network with activation spreading from right parieto-occipital scalp, to regions over right superior cortices (Foxe, McCourt, & Javitt, 2003). The right hemisphere may also control shifts in attention when viewing a scene - fMRI studies have reported right-lateralized fronto-parietal activity during shifts in visual attention (Corbetta, Kincade, Ollinger, McAvoy, & Shulman, 2000). Furthermore, a recent EEG study found increased processing of optic flow speed over right parietal recording sites (Vilhelmsen, van der Weel, & van der Meer, 2015). And in an older study that used positron emission tomography (PET), the right precuneus was cited as one of three areas that showed increased

cerebral blood flow specifically in response to optic flow stimulation (de Jong, Shipp, Skidmore, Frackowiak, & Zeki, 1994). These authors claim that both dorsal and ventral pathways are involved in the processing of optic flow stimuli, based on their finding of occipito-parietal as well as occipito-temporal activation patterns (de Jong et al., 1994). This claim is in line with a recent proposal that the inferior parietal lobe does not fit into the traditional dorsal-ventral visual processing stream dichotomy, and that specifically the right inferior parietal lobe plays an important role in maintaining attention while also responding to salient new information (Singh-Curry & Husain, 2009).

Supplementary motor area (SMA)

The SMA has been implicated in an enormous variety of motor functions including planning and gait initiation (Mihara, Miyai, Hatakenaka, Kubota, & Sakoda, 2007) and coordinating more demanding walking tasks (Kurz, Wilson, & Arpin, 2012), as well as cognitive control functions (Nachev, Kennard, & Husain, 2008). In a recent MoBI study employing connectivity analysis based on fluctuations in spectral power between cortical IC clusters, the authors proposed a cortical network underlying both active and viewed limb movements driven by the right premotor cortex and SMA, but also including cingulate and parietal areas (Kline et al., 2016). In another MoBI paradigm, brain-to-muscle connectivity was assessed by measuring heel-strike related spectral perturbations and electromyographic recordings (Artoni et al., 2017). They found evidence of unidirectional drive from contralateral motor cortex to leg muscles in the swing phase, with stronger modulations in mu, beta and gamma bands for clusters over motor areas compared to non-motor areas. And motor regions, including the cingulate motor cortex, supplementary motor area, and primary foot motor cortex were among the cortical areas with maximal influence on lower limb muscles during stereotyped walking (Artoni et al., 2017).

Therefore it does not come as a surprise that we also observed modulatory activity resulting from both sensory and cognitive processing in this cluster. A desynchronization was

observed in both alpha and beta bands associated with increased visual input (optic flow), compared to the static condition. Additionally, theta power was significantly reduced with MLP, in comparison to the other visual conditions. Furthermore, an interaction was observed for alpha frequencies, as the presentation of ML perturbations resulted in a different pattern of spectral modulation depending on whether one was engaged in the task or not. Finally, in relation to cognitive load, theta power was higher when participants performed the task; in line with findings showing theta power is sensitive to the recruitment of executive control in interference situations (Nigbur, Ivanova, & Sturmer, 2011).

Anterior cingulate cortex (ACC)

According to fMRI studies, the ACC is thought to monitor ongoing mental processes and signal the need for increased attentional focus (Fassbender et al., 2009; O'Connell et al., 2007; Simoes-Franklin, Hester, Shpaner, Foxe, & Garavan, 2010). We observed significant increases in theta and alpha spectral power in this cluster, observed across approximately 3-12Hz frequencies, for the static visual condition compared to both dynamic optic flow conditions. Additionally, theta power showed a significant increase for task performance, in line with the results observed in the SMA cluster above, and points to the role of theta oscillations in executive control processes during increased task load (Clayton et al., 2015). Cognitive-task related modulations in this cluster likely reflect processing demands dedicated to the Go/No-Go task, as the ACC has frequently been cited for recruitment in processing error detection and correction (O'Connell et al., 2007; Walton, Croxson, Behrens, Kennerley, & Rushworth, 2007) as well as evidence from a Go/No-Go ERP study implicating this area in conflict monitoring and attentional allocation (Dias, Foxe, & Javitt, 2003; Fallgatter, Bartsch, & Herrmann, 2002).

In conclusion, by utilizing an ICA and clustering approach to isolate cortical sources supporting dual-task walking activity, we have demonstrated that the MoBI technique is capable

of distinguishing subtle modulations in gait and spectral power attributed to sensory and cognitive load. Future investigations will examine event-related spectral perturbations (ERSPs) to determine if the timing of spectral power fluctuations is associated with specific phases of the gait cycle. This will add to the literature as cortical involvement in gait is already being explored in the context of steady-state and robotic-assisted treadmill walking (Gwin et al., 2011; Presacco et al., 2012; Seeber, Scherer, Wagner, Solis-Escalante, & Muller-Putz, 2014; Wagner et al., 2016; Wagner et al., 2012). In future MoBI protocols, the utilization of spatially-filtered EEG signals during active movements may provide insight into the neural dynamics underlying gait adaptation. This area of research is especially relevant for applications such as neurorehabilitation, for example to decode user intentions from EEG in brain-computer interfaces (Kilicarslan, Prasad, Grossman, & Contreras-Vidal, 2013; Wagner et al., 2012). Additionally, valuable information may be gained in relation to monitoring the neural correlates underlying disease progression and rehabilitation in diseases such as Multiple Sclerosis and Parkinson's (Boyd, Vidoni, & Daly, 2007). Finally, older adults often have difficulty adapting to increased cognitive load during locomotion and show evidence of declines in proprioceptive, vestibular and somatosensory processing (Goble, Coxon, Wenderoth, Van Impe, & Swinnen, 2009; Hay, Bard, Fleury, & Teasdale, 1996), factors that may increase fall risk (Ayers, Tow, Holtzer, & Verghese, 2014; Setti, Burke, Kenny, & Newell, 2011). MoBI approaches in virtual reality environments (e.g., visual perturbations) could be employed in combination with gait training strategies to successfully challenge people's walking ability, with the aim of reducing fall risk in vulnerable populations.

Acknowledgments

The primary source of funding for this work was provided by a pilot grant from the Einstein-Montefiore Institute for Clinical and Translational Research (UL1-TR000086) and the Sheryl & Daniel R. Tishman Charitable Foundation. Participant recruitment and scheduling were performed by the Human Clinical Phenotyping Core at Einstein, a facility of the Rose F. Kennedy Intellectual and Developmental Disabilities Research Center (RFK-IDDRC) which is funded by a center grant from the Eunice Kennedy Shriver National Institute of Child Health & Human Development (NICHD P30 HD071593). We would like to express our sincere gratitude to the participants for giving their time to this effort.

Figure 1: Representation of recording apparatus: a participant walking on the treadmill wearing an EEG cap and motion capture markers, facing the optic flow display.

Figure 2: Response inhibition performance on the Go/No-Go task. From left to right: percentage of correct rejections (CRs) for all 16 participants during static visual field, dynamic optic flow with no perturbation (NOP) and optic flow with ML perturbation (MLP). Red markers indicate the means for each condition, with vertical bars representing standard deviations.

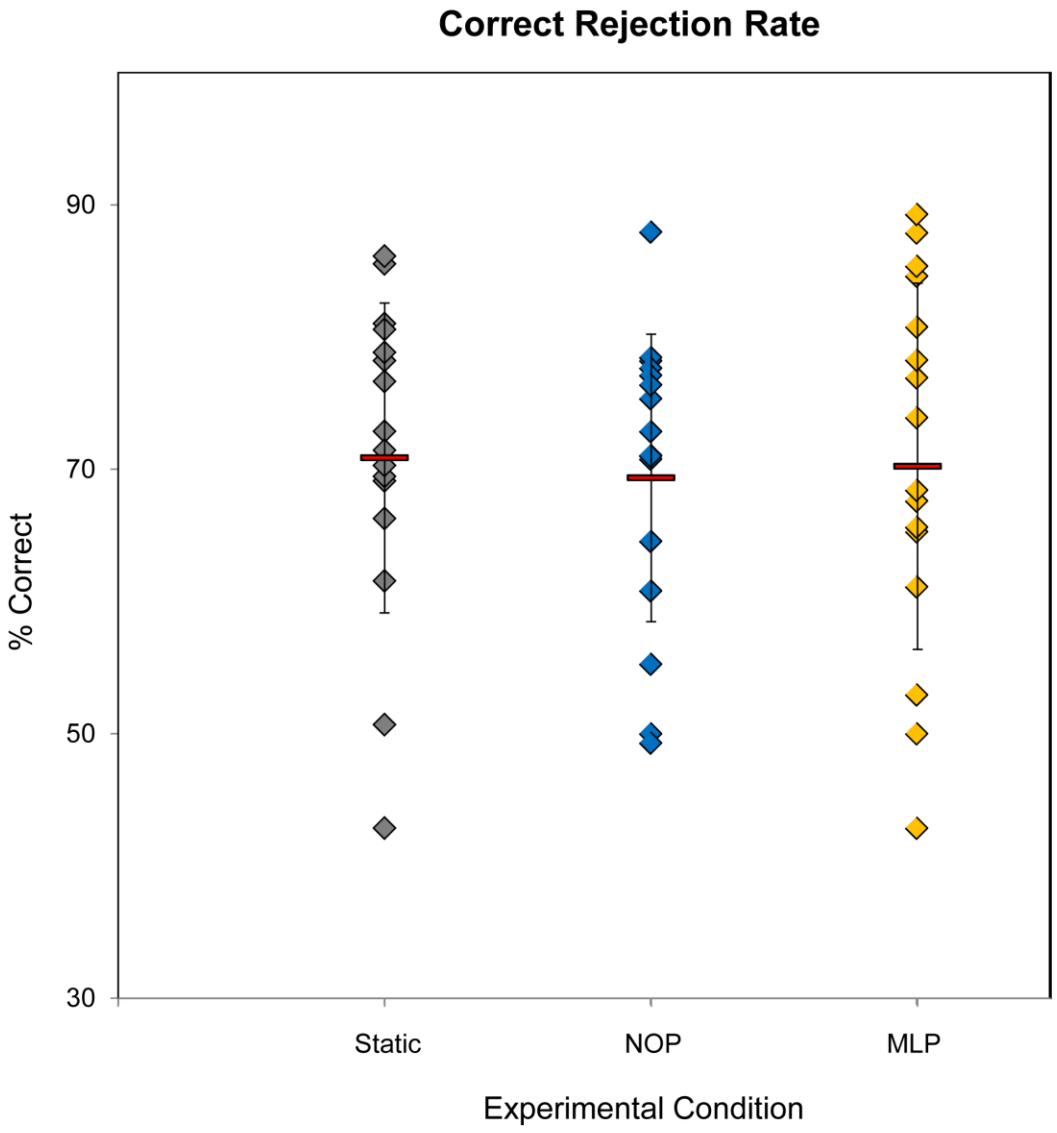

Figure 3: Average and mean variability for stride time, stride length and step width. Top row represents means, bottom row is mean SD, for stride time (left column), stride length (center) and step width (right column) for all six experimental conditions. Open circles represent the No-Task conditions, while crosses represent Task blocks. S_{NT} = Static No Task, NOP_{NT} = No perturbation No Task, MLP_{NT} = Mediolateral perturbation No Task, S_T = Static Task, NOP_T = No perturbation Task, MLP_T = Mediolateral perturbation Task.

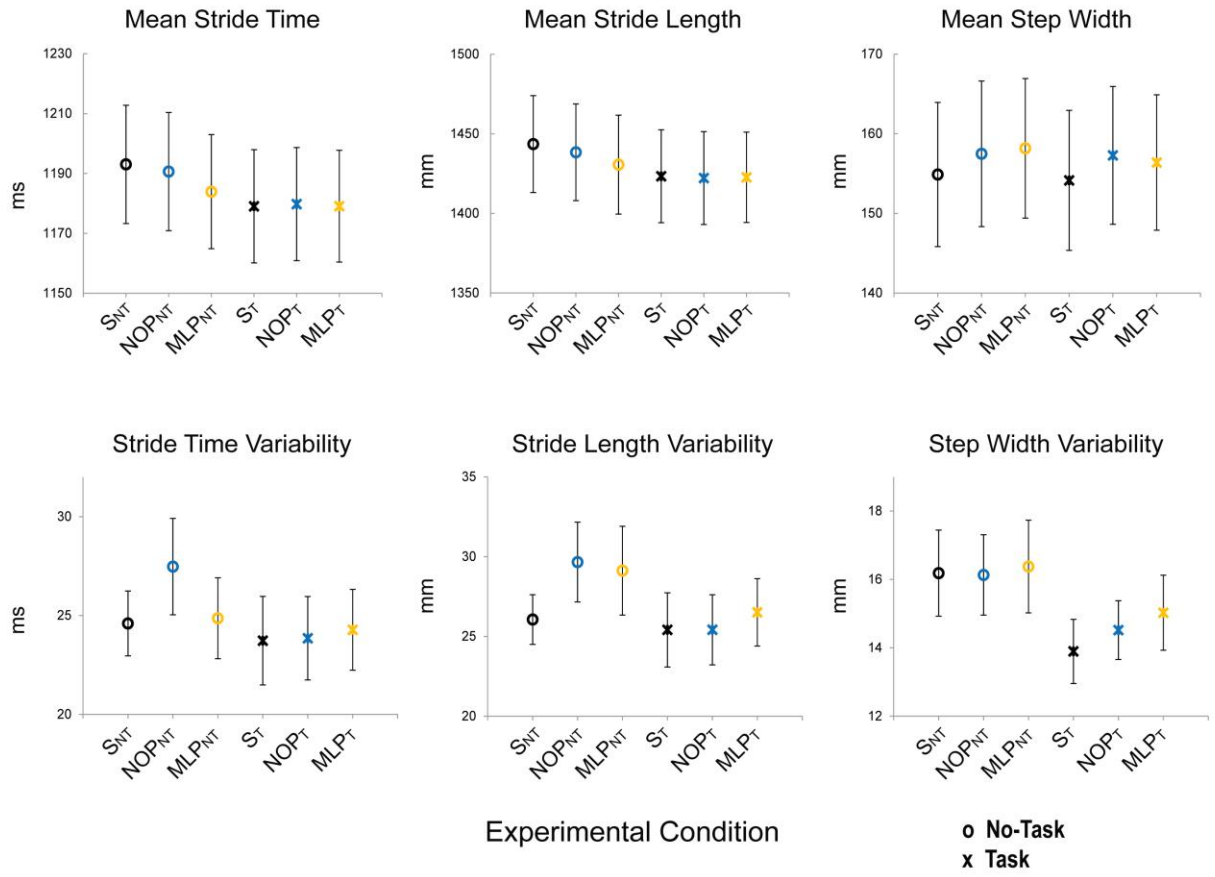

Figure 4: Average variability in head position, in ML (left) and AP (right) directions for all six experimental conditions. Open circles represent the No-Task conditions, while crosses represent Task blocks. S_{NT} = Static No Task, NOP_{NT} = No perturbation No Task, MLP_{NT} = Mediolateral perturbation No Task, S_T = Static Task, NOP_T = No perturbation Task, MLP_T = Mediolateral perturbation Task.

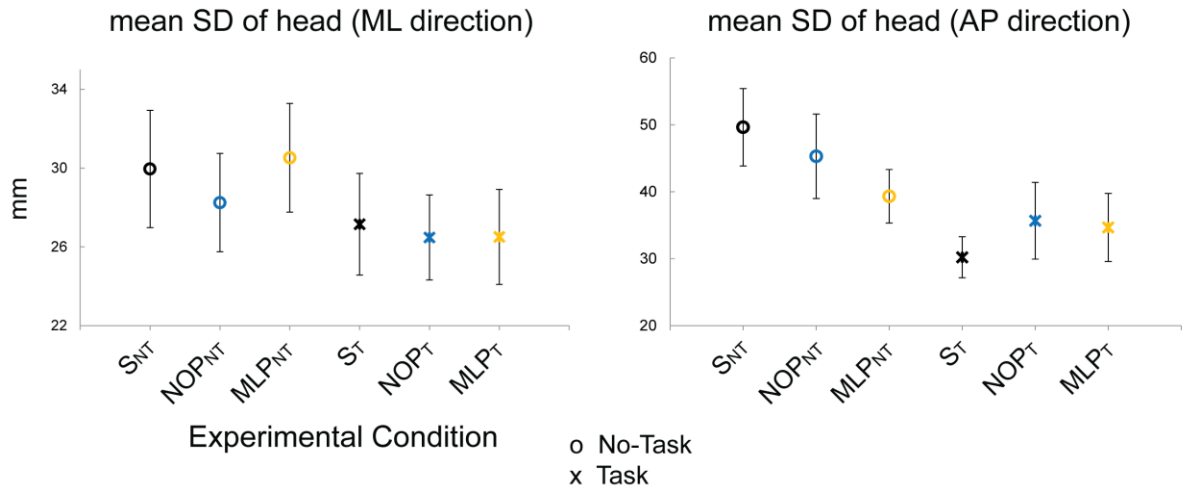

Table 1: Clusters of Independent electrocortical sources (ICs). Description and approximate location (Brodmann area and Tailarach coordinates) of cluster centroids for all clusters located in the cortex and containing ICs from more than half of the participants.

Functional Area	Brodmann Area	Talairach coordinates (x,y,z)	No. of subjects (S) and ICs
Medial occipital lobe, lingual gyrus	BA17	11, -94, -10	12 S, 14 ICs
Right occipital	BA19	47, -73, -1	11 S, 12 ICs
Left occipital	BA19	-43, -71, 14	12 S, 14 ICs
Left superior temporal gyrus	BA22	-47, -17, -6	10 S, 12 ICs
Right inferior parietal lobule	BA40	43, -34, 36	8 S, 10 ICs
Parietal lobe, precuneus	BA7	12, -62, 34	11 S, 15 ICs
Supplementary motor area	BA6	-6, -16, 45	14 S, 23 ICs
Limbic lobe, anterior cingulate	BA24	1, 25, 22	14 S, 15 ICs

Figure 5: Clusters of electrocortical sources localized to occipital cortex (yellow), parietal cortex (inferior parietal lobule: cyan, precuneus: red) and frontal cortex (Supplementary Motor Area: purple, Anterior Cingulate Cortex: green).

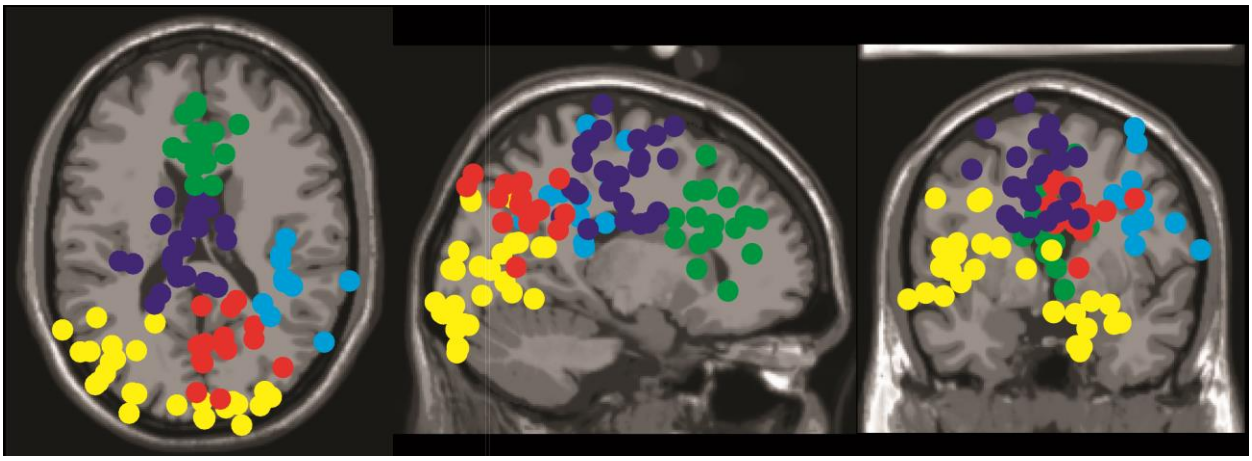

Figure 6: Occipital cortex clusters. Scalp topography, dipole location (blue dots indicate the location of each IC, red dots represent the cluster centroid) and average power spectral density.

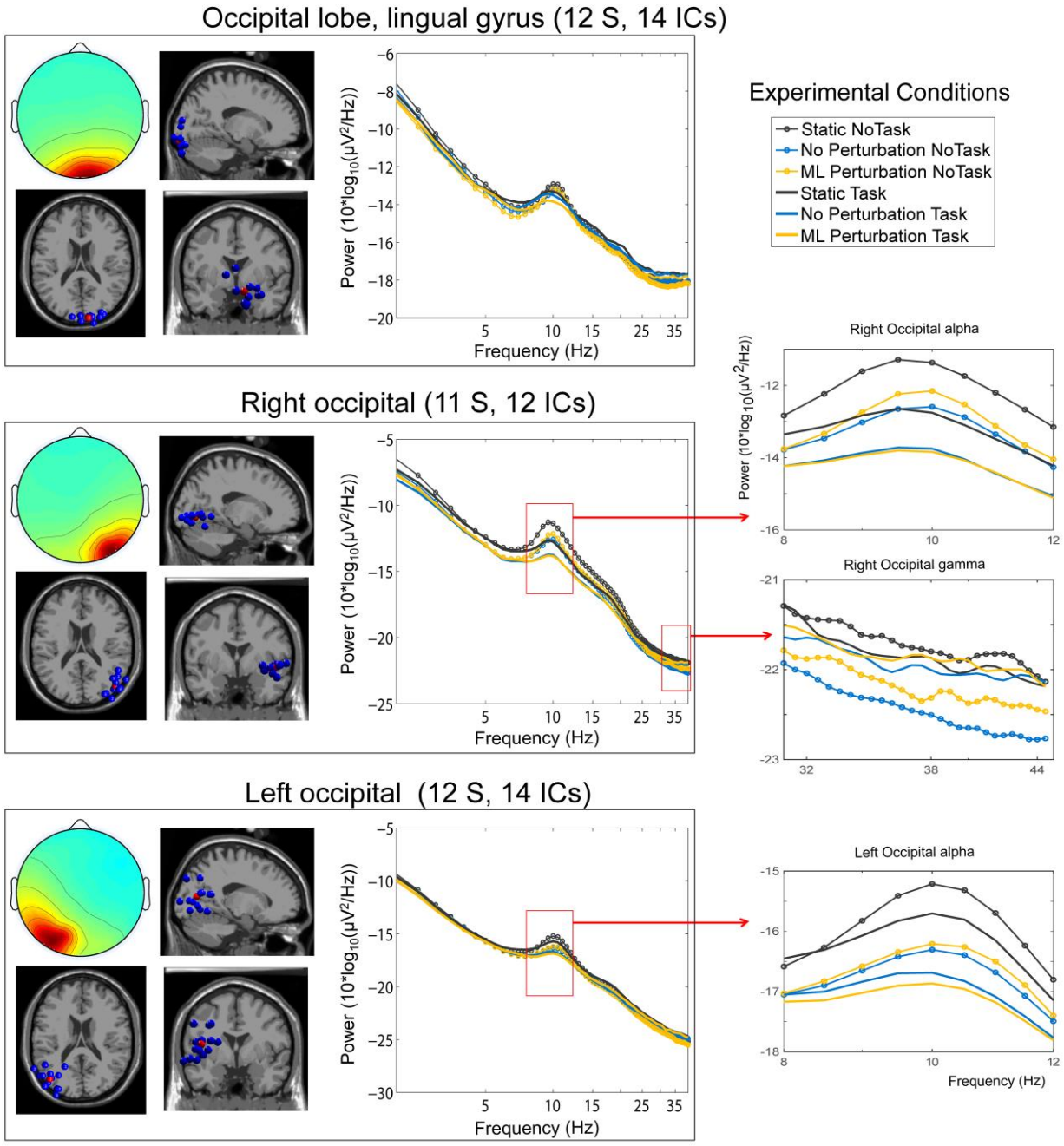

Figure 7: Clusters located over temporal and parietal cortex. Scalp topography, dipole location (blue dots indicate the location of each IC, red dots represent the cluster centroid) and average power spectral density.

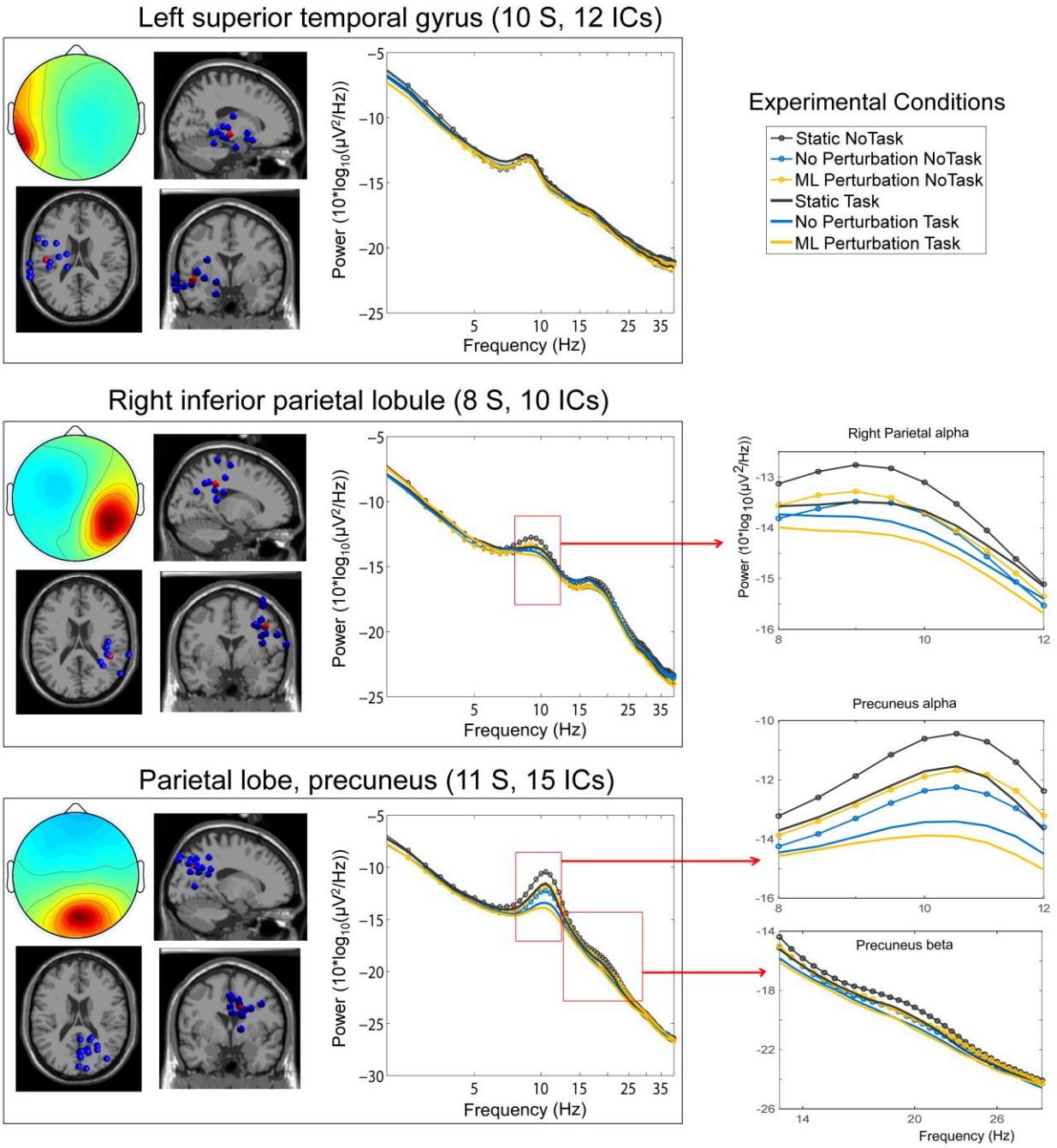

Figure 8: Clusters located over frontal cortical areas. Scalp topography, dipole location (blue dots indicate the location of each IC, red dots represent the cluster centroid) and average power spectral density for the cluster localized to the supplementary motor area (top panel) and the anterior cingulate (bottom panel).

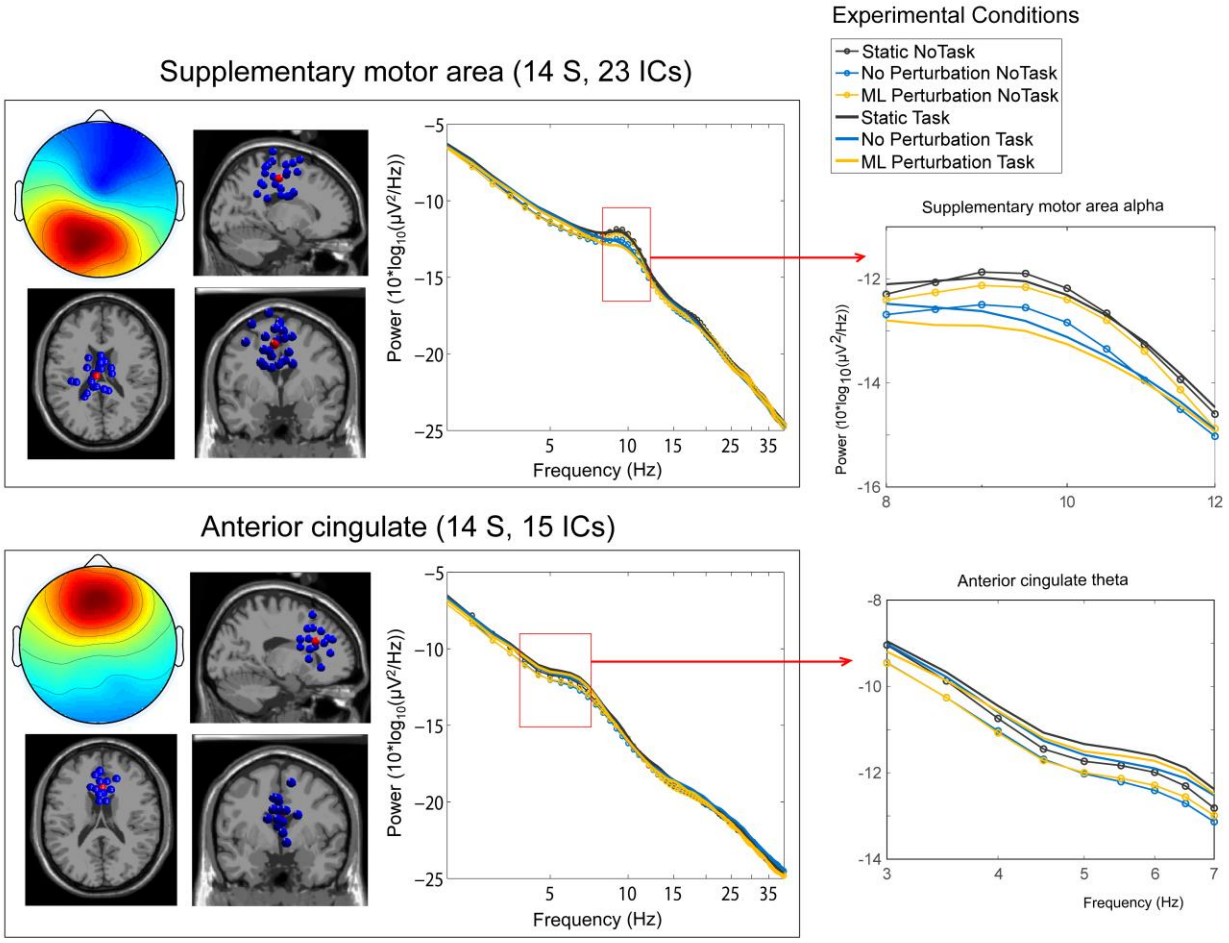

REFERENCES

Akalin Acar, Z., & Makeig, S. (2013). Effects of forward model errors on EEG source localization. *Brain Topogr, 26*(3), 378-396. doi: 10.1007/s10548-012-0274-6

Al-Yahya, E., Dawes, H., Smith, L., Dennis, A., Howells, K., & Cockburn, J. (2011). Cognitive motor interference while walking: a systematic review and meta-analysis. *Neurosci Biobehav Rev, 35*(3), 715-728. doi: 10.1016/j.neubiorev.2010.08.008

Alton, F., Baldey, L., Caplan, S., & Morrissey, M. C. (1998). A kinematic comparison of overground and treadmill walking. *Clin Biomech (Bristol, Avon), 13*(6), 434-440.

Artoni, F., Fanciullacci, C., Bertolucci, F., Panarese, A., Makeig, S., Micera, S., & Chisari, C. (2017). Unidirectional brain to muscle connectivity reveals motor cortex control of leg muscles during stereotyped walking. *Neuroimage, 159*, 403-416. doi: 10.1016/j.neuroimage.2017.07.013

Ayers, E. I., Tow, A. C., Holtzer, R., & Verghese, J. (2014). Walking while talking and falls in aging. *Gerontology, 60*(2), 108-113. doi: 10.1159/000355119

Bakker, M., De Lange, F. P., Helmich, R. C., Scheeringa, R., Bloem, B. R., & Toni, I. (2008). Cerebral correlates of motor imagery of normal and precision gait. *Neuroimage, 41*(3), 998-1010. doi: 10.1016/j.neuroimage.2008.03.020

Banerjee, S., Snyder, A. C., Molholm, S., & Foxe, J. J. (2011). Oscillatory alpha-band mechanisms and the deployment of spatial attention to anticipated auditory and visual target locations: supramodal or sensory-specific control mechanisms? *J Neurosci, 31*(27), 9923-9932. doi: 10.1523/JNEUROSCI.4660-10.2011

Ble, A., Volpato, S., Zuliani, G., Guralnik, J. M., Bandinelli, S., Lauretani, F., . . . Ferrucci, L. (2005). Executive function correlates with walking speed in older persons: the InCHIANTI study. *J Am Geriatr Soc, 53*(3), 410-415. doi: 10.1111/j.1532-5415.2005.53157.x

Boyd, L. A., Vidoni, E. D., & Daly, J. J. (2007). Answering the call: the influence of neuroimaging and electrophysiological evidence on rehabilitation. *Phys Ther, 87*(6), 684-703. doi: 10.2522/ptj.20060164

Brady, R. A., Peters, B. T., & Bloomberg, J. J. (2009). Strategies of healthy adults walking on a laterally oscillating treadmill. *Gait Posture, 29*(4), 645-649. doi: 10.1016/j.gaitpost.2009.01.010

Butler, J. S., Smith, S. T., Campos, J. L., & Bulthoff, H. H. (2010). Bayesian integration of visual and vestibular signals for heading. *J Vis, 10*(11), 23. doi: 10.1167/10.11.23

Castermans, T., Duvinage, M., Cheron, G., & Dutoit, T. (2014). About the cortical origin of the low-delta and high-gamma rhythms observed in EEG signals during treadmill walking. *Neurosci Lett, 561*, 166-170. doi: 10.1016/j.neulet.2013.12.059

Cavanna, A. E., & Trimble, M. R. (2006). The precuneus: a review of its functional anatomy and behavioural correlates. *Brain, 129*(Pt 3), 564-583. doi: 10.1093/brain/awl004

Cevallos, C., Zarka, D., Hoellinger, T., Leroy, A., Dan, B., & Cheron, G. (2015). Oscillations in the human brain during walking execution, imagination and observation. *Neuropsychologia, 79*(Pt B), 223-232. doi: 10.1016/j.neuropsychologia.2015.06.039

Clayton, M. S., Yeung, N., & Cohen Kadosh, R. (2015). The roles of cortical oscillations in sustained attention. *Trends Cogn Sci, 19*(4), 188-195. doi: 10.1016/j.tics.2015.02.004

Corbetta, M., Kincade, J. M., Ollinger, J. M., McAvoy, M. P., & Shulman, G. L. (2000). Voluntary orienting is dissociated from target detection in human posterior parietal cortex. *Nat Neurosci, 3*(3), 292-297. doi: 10.1038/73009

de Jong, B. M., Shipp, S., Skidmore, B., Frackowiak, R. S., & Zeki, S. (1994). The cerebral activity related to the visual perception of forward motion in depth. *Brain, 117 (Pt 5)*, 1039-1054.

1008 De Sanctis, P., Butler, J. S., Green, J. M., Snyder, A. C., & Foxe, J. J. (2012). Mobile brain/body
1009 imaging (MoBI): High-density electrical mapping of inhibitory processes during walking.
1010 *Conf Proc IEEE Eng Med Biol Soc, 2012*, 1542-1545. doi: 10.1109/EMBC.2012.6346236
1011 De Sanctis, P., Butler, J. S., Malcolm, B. R., & Foxe, J. J. (2014). Recalibration of inhibitory
1012 control systems during walking-related dual-task interference: a mobile brain-body
1013 imaging (MOBI) study. *Neuroimage, 94*, 55-64. doi: 10.1016/j.neuroimage.2014.03.016
1014 De Vos, M., Gandras, K., & Debener, S. (2014). Towards a truly mobile auditory brain-computer
1015 interface: exploring the P300 to take away. *Int J Psychophysiol, 91*(1), 46-53. doi:
1016 10.1016/j.ijpsycho.2013.08.010
1017 Delaney, H. D., & Maxwell, S. E. (1981). On Using Analysis Of Covariance In Repeated
1018 Measures Designs. *Multivariate Behav Res, 16*(1), 105-123. doi:
1019 10.1207/s15327906mbr1601_6
1020 Delorme, A., & Makeig, S. (2004). EEGLAB: an open source toolbox for analysis of single-trial
1021 EEG dynamics including independent component analysis. *J Neurosci Methods, 134*(1),
1022 9-21. doi: 10.1016/j.jneumeth.2003.10.009
1023 Delorme, A., Palmer, J., Onton, J., Oostenveld, R., & Makeig, S. (2012). Independent EEG
1024 sources are dipolar. *PLoS One, 7*(2), e30135. doi: 10.1371/journal.pone.0030135
1025 Delorme, A., Sejnowski, T., & Makeig, S. (2007). Enhanced detection of artifacts in EEG data
1026 using higher-order statistics and independent component analysis. *Neuroimage, 34*(4),
1027 1443-1449. doi: 10.1016/j.neuroimage.2006.11.004
1028 Dias, E. C., Foxe, J. J., & Javitt, D. C. (2003). Changing plans: a high density electrical mapping
1029 study of cortical control. *Cereb Cortex, 13*(7), 701-715.
1030 Dingwell, J. B., & Cusumano, J. P. (2015). Identifying stride-to-stride control strategies in human
1031 treadmill walking. *PLoS One, 10*(4), e0124879. doi: 10.1371/journal.pone.0124879

1032 Dingwell, J. B., John, J., & Cusumano, J. P. (2010). Do humans optimally exploit redundancy to
1033 control step variability in walking? *PLoS Comput Biol, 6*(7), e1000856. doi:
1034 10.1371/journal.pcbi.1000856
1035 Dockree, P. M., Kelly, S. P., Foxe, J. J., Reilly, R. B., & Robertson, I. H. (2007). Optimal
1036 sustained attention is linked to the spectral content of background EEG activity: greater
1037 ongoing tonic alpha (approximately 10 Hz) power supports successful phasic goal
1038 activation. *Eur J Neurosci, 25*(3), 900-907. doi: 10.1111/j.1460-9568.2007.05324.x
1039 Duffy, C. J., & Wurtz, R. H. (1991). Sensitivity of MST neurons to optic flow stimuli. II.
1040 Mechanisms of response selectivity revealed by small-field stimuli. *J Neurophysiol,*
1041 *65*(6), 1346-1359.
1042 Duysens, J., & Van de Crommert, H. W. (1998). Neural control of locomotion; The central
1043 pattern generator from cats to humans. *Gait Posture, 7*(2), 131-141.
1044 Fallgatter, A. J., Bartsch, A. J., & Herrmann, M. J. (2002). Electrophysiological measurements of
1045 anterior cingulate function. *J Neural Transm (Vienna), 109*(5-6), 977-988. doi:
1046 10.1007/s007020200080
1047 Fassbender, C., Hester, R., Murphy, K., Foxe, J. J., Foxe, D. M., & Garavan, H. (2009).
1048 Prefrontal and midline interactions mediating behavioural control. *Eur J Neurosci, 29*(1),
1049 181-187. doi: 10.1111/j.1460-9568.2008.06557.x
1050 Fitzgibbon, S. P., Pope, K. J., Mackenzie, L., Clark, C. R., & Willoughby, J. O. (2004). Cognitive
1051 tasks augment gamma EEG power. *Clin Neurophysiol, 115*(8), 1802-1809. doi:
1052 10.1016/j.clinph.2004.03.009
1053 Foxe, J. J., McCourt, M. E., & Javitt, D. C. (2003). Right hemisphere control of visuospatial
1054 attention: line-bisection judgments evaluated with high-density electrical mapping and
1055 source analysis. *Neuroimage, 19*(3), 710-726.

1056 Foxe, J. J., Simpson, G. V., & Ahlfors, S. P. (1998). Parieto-occipital approximately 10 Hz
1057 activity reflects anticipatory state of visual attention mechanisms. *Neuroreport, 9*(17),
1058 3929-3933.
1059 Foxe, J. J., & Snyder, A. C. (2011). The Role of Alpha-Band Brain Oscillations as a Sensory
1060 Suppression Mechanism during Selective Attention. *Front Psychol, 2*, 154. doi:
1061 10.3389/fpsyg.2011.00154
1062 Goble, D. J., Coxon, J. P., Wenderoth, N., Van Impe, A., & Swinnen, S. P. (2009).
1063 Proprioceptive sensibility in the elderly: degeneration, functional consequences and
1064 plastic-adaptive processes. *Neurosci Biobehav Rev, 33*(3), 271-278. doi:
1065 10.1016/j.neubiorev.2008.08.012
1066 Grabiner, M. D., & Troy, K. L. (2005). Attention demanding tasks during treadmill walking reduce
1067 step width variability in young adults. *J Neuroeng Rehabil, 2*, 25. doi: 10.1186/1743-
1068 0003-2-25
1069 Gramann, K., Gwin, J. T., Bigdely-Shamlo, N., Ferris, D. P., & Makeig, S. (2010). Visual evoked
1070 responses during standing and walking. *Front Hum Neurosci, 4*, 202. doi:
1071 10.3389/fnhum.2010.00202
1072 Gramann, K., Gwin, J. T., Ferris, D. P., Oie, K., Jung, T. P., Lin, C. T., . . . Makeig, S. (2011).
1073 Cognition in action: imaging brain/body dynamics in mobile humans. *Rev Neurosci,*
1074 *22*(6), 593-608. doi: 10.1515/RNS.2011.047
1075 Gramann, K., Jung, T. P., Ferris, D. P., Lin, C. T., & Makeig, S. (2014). Toward a new cognitive
1076 neuroscience: modeling natural brain dynamics. *Front Hum Neurosci, 8*, 444. doi:
1077 10.3389/fnhum.2014.00444
1078 Grillner, S., Wallen, P., Saitoh, K., Kozlov, A., & Robertson, B. (2008). Neural bases of goal-
1079 directed locomotion in vertebrates--an overview. *Brain Res Rev, 57*(1), 2-12. doi:
1080 10.1016/j.brainresrev.2007.06.027

Gwin, J. T., Gramann, K., Makeig, S., & Ferris, D. P. (2010). Removal of movement artifact from high-density EEG recorded during walking and running. *J Neurophysiol, 103*(6), 3526-3534. doi: 10.1152/jn.00105.2010

Gwin, J. T., Gramann, K., Makeig, S., & Ferris, D. P. (2011). Electrocortical activity is coupled to gait cycle phase during treadmill walking. *Neuroimage, 54*(2), 1289-1296. doi: 10.1016/j.neuroimage.2010.08.066

Harada, T., Miyai, I., Suzuki, M., & Kubota, K. (2009). Gait capacity affects cortical activation patterns related to speed control in the elderly. *Exp Brain Res, 193*(3), 445-454. doi: 10.1007/s00221-008-1643-y

Harris, I. M., Egan, G. F., Sonkkila, C., Tochon-Danguy, H. J., Paxinos, G., & Watson, J. D. (2000). Selective right parietal lobe activation during mental rotation: a parametric PET study. *Brain, 123 (Pt 1)*, 65-73.

Hay, L., Bard, C., Fleury, M., & Teasdale, N. (1996). Availability of visual and proprioceptive afferent messages and postural control in elderly adults. *Exp Brain Res, 108*(1), 129-139.

Hollman, J. H., Brey, R. H., Robb, R. A., Bang, T. J., & Kaufman, K. R. (2006). Spatiotemporal gait deviations in a virtual reality environment. *Gait Posture, 23*(4), 441-444. doi: 10.1016/j.gaitpost.2005.05.005

Hollman, J. H., Kovash, F. M., Kubik, J. J., & Linbo, R. A. (2007). Age-related differences in spatiotemporal markers of gait stability during dual task walking. *Gait Posture, 26*(1), 113-119. doi: 10.1016/j.gaitpost.2006.08.005

Jacobs, J. V., & Horak, F. B. (2007). Cortical control of postural responses. *J Neural Transm, 114*(10), 1339-1348. doi: 10.1007/s00702-007-0657-0

Joseph, R. (1988). The Right Cerebral Hemisphere - Emotion, Music, Visual-Spatial Skills, Body-Image, Dreams, and Awareness. *J Clin Psychol, 44*(5), 630-673. doi: Doi 10.1002/1097-4679(198809)44:5<630::Aid-Jclp2270440502>3.0.Co;2-V

Jung, T. P., Makeig, S., Westerfield, M., Townsend, J., Courchesne, E., & Sejnowski, T. J. (2000). Removal of eye activity artifacts from visual event-related potentials in normal and clinical subjects. *Clinical Neurophysiology, 111*(10), 1745-1758. doi: Doi 10.1016/S1388-2457(00)00386-2

Kang, H. G., & Dingwell, J. B. (2008). Separating the effects of age and walking speed on gait variability. *Gait Posture, 27*(4), 572-577. doi: 10.1016/j.gaitpost.2007.07.009

Kelly, S. P., Lalor, E. C., Reilly, R. B., & Foxe, J. J. (2006). Increases in alpha oscillatory power reflect an active retinotopic mechanism for distracter suppression during sustained visuospatial attention. *J Neurophysiol, 95*(6), 3844-3851. doi: 10.1152/jn.01234.2005

Kilicarslan, A., Prasad, S., Grossman, R. G., & Contreras-Vidal, J. L. (2013). High accuracy decoding of user intentions using EEG to control a lower-body exoskeleton. *Conf Proc IEEE Eng Med Biol Soc, 2013*, 5606-5609. doi: 10.1109/EMBC.2013.6610821

Klimesch, W. (2012). alpha-band oscillations, attention, and controlled access to stored information. *Trends Cogn Sci, 16*(12), 606-617. doi: 10.1016/j.tics.2012.10.007

Kline, J. E., Huang, H. J., Snyder, K. L., & Ferris, D. P. (2015). Isolating gait-related movement artifacts in electroencephalography during human walking. *J Neural Eng, 12*(4), 046022. doi: 10.1088/1741-2560/12/4/046022

Kline, J. E., Huang, H. J., Snyder, K. L., & Ferris, D. P. (2016). Cortical Spectral Activity and Connectivity during Active and Viewed Arm and Leg Movement. *Front Neurosci, 10*, 91. doi: 10.3389/fnins.2016.00091

Kline, J. E., Poggensee, K., & Ferris, D. P. (2014). Your brain on speed: cognitive performance of a spatial working memory task is not affected by walking speed. *Front Hum Neurosci, 8*, 288. doi: 10.3389/fnhum.2014.00288

Kurz, M. J., Wilson, T. W., & Arpin, D. J. (2012). Stride-time variability and sensorimotor cortical activation during walking. *Neuroimage, 59*(2), 1602-1607. doi: 10.1016/j.neuroimage.2011.08.084

Lappe, M., Bremmer, F., & van den Berg, A. V. (1999). Perception of self-motion from visual flow. *Trends in Cognitive Sciences, 3*(9), 329-336. doi: Doi 10.1016/S1364-6613(99)01364-9

Lappe, M., & Grigo, A. (1999). How stereovision interacts with optic flow perception: neural mechanisms. *Neural Netw, 12*(9), 1325-1329.

Lovden, M., Schaefer, S., Pohlmeyer, A. E., & Lindenberger, U. (2008). Walking variability and working-memory load in aging: a dual-process account relating cognitive control to motor control performance. *J Gerontol B Psychol Sci Soc Sci, 63*(3), P121-128.

Makeig, S., Bell, A. J., Jung, T. P., & Sejnowski, T. J. (1996). Independent component analysis of electroencephalographic data. . *Advances in Neural Information Processing Systems, 8*, 145-151.

Makeig, S., Gramann, K., Jung, T. P., Sejnowski, T. J., & Poizner, H. (2009). Linking brain, mind and behavior. *Int J Psychophysiol, 73*(2), 95-100. doi: 10.1016/j.ijpsycho.2008.11.008

Malcolm, B. R., Foxe, J. J., Butler, J. S., & De Sanctis, P. (2015). The aging brain shows less flexible reallocation of cognitive resources during dual-task walking: A mobile brain/body imaging (MoBI) study. *Neuroimage, 117*, 230-242. doi: 10.1016/j.neuroimage.2015.05.028

Malcolm, B. R., Foxe, J. J., Butler, J. S., Mowrey, W. B., Molholm, S., & De Sanctis, P. (2017). Long-term test-retest reliability of event-related potential (ERP) recordings during treadmill walking using the mobile brain/body imaging (MoBI) approach. *Brain Res*. doi: 10.1016/j.brainres.2017.05.021

McAndrew, P. M., Dingwell, J. B., & Wilken, J. M. (2010). Walking variability during continuous pseudo-random oscillations of the support surface and visual field. *J Biomech, 43*(8), 1470-1475. doi: 10.1016/j.jbiomech.2010.02.003

McAndrew, P. M., Wilken, J. M., & Dingwell, J. B. (2011). Dynamic stability of human walking in visually and mechanically destabilizing environments. *J Biomech, 44*(4), 644-649. doi: 10.1016/j.jbiomech.2010.11.007

Mihara, M., Miyai, I., Hatakenaka, M., Kubota, K., & Sakoda, S. (2007). Sustained prefrontal activation during ataxic gait: a compensatory mechanism for ataxic stroke? *Neuroimage, 37*(4), 1338-1345. doi: 10.1016/j.neuroimage.2007.06.014

Miyai, I., Tanabe, H. C., Sase, I., Eda, H., Oda, I., Konishi, I., . . . Kubota, K. (2001). Cortical mapping of gait in humans: a near-infrared spectroscopic topography study. *Neuroimage, 14*(5), 1186-1192. doi: 10.1006/nimg.2001.0905

Mullen, T., Acar, Z. A., Worrell, G., & Makeig, S. (2011). Modeling cortical source dynamics and interactions during seizure. *Conf Proc IEEE Eng Med Biol Soc, 2011*, 1411-1414. doi: 10.1109/IEMBS.2011.6090332

Nachev, P., Kennard, C., & Husain, M. (2008). Functional role of the supplementary and pre-supplementary motor areas. *Nat Rev Neurosci, 9*(11), 856-869. doi: 10.1038/nrn2478

Nathan, K., & Contreras-Vidal, J. L. (2015). Negligible Motion Artifacts in Scalp Electroencephalography (EEG) During Treadmill Walking. *Front Hum Neurosci, 9*, 708. doi: 10.3389/fnhum.2015.00708

Nigbur, R., Ivanova, G., & Sturmer, B. (2011). Theta power as a marker for cognitive interference. *Clin Neurophysiol, 122*(11), 2185-2194. doi: 10.1016/j.clinph.2011.03.030

O'Connell, R. G., Dockree, P. M., Bellgrove, M. A., Kelly, S. P., Hester, R., Garavan, H., . . . Foxe, J. J. (2007). The role of cingulate cortex in the detection of errors with and without awareness: a high-density electrical mapping study. *Eur J Neurosci, 25*(8), 2571-2579. doi: 10.1111/j.1460-9568.2007.05477.x

O'Connor, S. M., & Kuo, A. D. (2009). Direction-dependent control of balance during walking and standing. *J Neurophysiol, 102*(3), 1411-1419. doi: 10.1152/jn.00131.2009

O'Shea, S., Morris, M. E., & Iansek, R. (2002). Dual task interference during gait in people with Parkinson disease: effects of motor versus cognitive secondary tasks. *Phys Ther, 82*(9), 888-897.

Onton, J., & Makeig, S. (2006). Information-based modeling of event-related brain dynamics. *Prog Brain Res, 159*, 99-120. doi: 10.1016/S0079-6123(06)59007-7

Onton, J., Westerfield, M., Townsend, J., & Makeig, S. (2006). Imaging human EEG dynamics using independent component analysis. *Neurosci Biobehav Rev, 30*(6), 808-822. doi: 10.1016/j.neubiorev.2006.06.007

Oostenveld, R., & Oostendorp, T. F. (2002). Validating the boundary element method for forward and inverse EEG computations in the presence of a hole in the skull. *Hum Brain Mapp, 17*(3), 179-192. doi: 10.1002/hbm.10061

Owings, T. M., & Grabiner, M. D. (2004). Variability of step kinematics in young and older adults. *Gait Posture, 20*(1), 26-29. doi: 10.1016/s0966-6362(03)00088-2

Pashler, H. (1994). Dual-task interference in simple tasks: data and theory. *Psychol Bull, 116*(2), 220-244.

Petersen, N. T., Butler, J. E., Marchand-Pauvert, V., Fisher, R., Ledebt, A., Pyndt, H. S., . . . Nielsen, J. B. (2001). Suppression of EMG activity by transcranial magnetic stimulation in human subjects during walking. *J Physiol, 537*(Pt 2), 651-656.

Petersen, N. T., Pyndt, H. S., & Nielsen, J. B. (2003). Investigating human motor control by transcranial magnetic stimulation. *Exp Brain Res, 152*(1), 1-16. doi: 10.1007/s00221-003-1537-y

Petersen, T. H., Willerslev-Olsen, M., Conway, B. A., & Nielsen, J. B. (2012). The motor cortex drives the muscles during walking in human subjects. *J Physiol, 590*(Pt 10), 2443-2452. doi: 10.1113/jphysiol.2012.227397

Pfurtscheller, G. (2000). Spatiotemporal ERD/ERS patterns during voluntary movement and motor imagery. *Suppl Clin Neurophysiol, 53*, 196-198.

Pfurtscheller, G., Graimann, B., Huggins, J. E., Levine, S. P., & Schuh, L. A. (2003). Spatiotemporal patterns of beta desynchronization and gamma synchronization in corticographic data during self-paced movement. *Clin Neurophysiol, 114*(7), 1226-1236.

Pfurtscheller, G., & Klimesch, W. (1991). Event-related desynchronization during motor behavior and visual information processing. *Electroencephalogr Clin Neurophysiol Suppl, 42*, 58-65.

Pfurtscheller, G., & Lopes da Silva, F. H. (1999). Event-related EEG/MEG synchronization and desynchronization: basic principles. *Clin Neurophysiol, 110*(11), 1842-1857.

Pfurtscheller, G., Stancak, A., Jr., & Neuper, C. (1996). Event-related synchronization (ERS) in the alpha band--an electrophysiological correlate of cortical idling: a review. *Int J Psychophysiol, 24*(1-2), 39-46.

Presacco, A., Forrester, L. W., & Contreras-Vidal, J. L. (2012). Decoding intra-limb and inter-limb kinematics during treadmill walking from scalp electroencephalographic (EEG) signals. *IEEE Trans Neural Syst Rehabil Eng, 20*(2), 212-219. doi: 10.1109/TNSRE.2012.2188304

Presacco, A., Goodman, R., Forrester, L., & Contreras-Vidal, J. L. (2011). Neural decoding of treadmill walking from noninvasive electroencephalographic signals. *J Neurophysiol, 106*(4), 1875-1887. doi: 10.1152/jn.00104.2011

Prokop, T., Schubert, M., & Berger, W. (1997). Visual influence on human locomotion. Modulation to changes in optic flow. *Exp Brain Res, 114*(1), 63-70.

Rossignol, S., Dubuc, R., & Gossard, J. P. (2006). Dynamic sensorimotor interactions in locomotion. *Physiol Rev, 86*(1), 89-154. doi: 10.1152/physrev.00028.2005

Seeber, M., Scherer, R., Wagner, J., Solis-Escalante, T., & Muller-Putz, G. R. (2014). EEG beta suppression and low gamma modulation are different elements of human upright walking. *Front Hum Neurosci, 8*, 485. doi: 10.3389/fnhum.2014.00485

Setti, A., Burke, K. E., Kenny, R. A., & Newell, F. N. (2011). Is inefficient multisensory processing associated with falls in older people? *Exp Brain Res, 209*(3), 375-384. doi: 10.1007/s00221-011-2560-z

Severens, M., Nienhuis, B., Desain, P., & Duysens, J. (2012). Feasibility of measuring event related desynchronization with electroencephalography during walking. *Conf Proc IEEE Eng Med Biol Soc, 2012*, 2764-2767. doi: 10.1109/EMBC.2012.6346537

Siegel, M., Donner, T. H., Oostenveld, R., Fries, P., & Engel, A. K. (2007). High-frequency activity in human visual cortex is modulated by visual motion strength. *Cereb Cortex, 17*(3), 732-741. doi: 10.1093/cercor/bhk025

Simoes-Franklin, C., Hester, R., Shpaner, M., Foxe, J. J., & Garavan, H. (2010). Executive function and error detection: The effect of motivation on cingulate and ventral striatum activity. *Hum Brain Mapp, 31*(3), 458-469. doi: 10.1002/hbm.20879

Singh-Curry, V., & Husain, M. (2009). The functional role of the inferior parietal lobe in the dorsal and ventral stream dichotomy. *Neuropsychologia, 47*(6), 1434-1448. doi: 10.1016/j.neuropsychologia.2008.11.033

Sipp, A. R., Gwin, J. T., Makeig, S., & Ferris, D. P. (2013). Loss of balance during balance beam walking elicits a multifocal theta band electrocortical response. *J Neurophysiol, 110*(9), 2050-2060. doi: 10.1152/jn.00744.2012

Snyder, A. C., & Foxe, J. J. (2010). Anticipatory attentional suppression of visual features indexed by oscillatory alpha-band power increases: a high-density electrical mapping study. *J Neurosci, 30*(11), 4024-4032. doi: 10.1523/JNEUROSCI.5684-09.2010

Snyder, K. L., Kline, J. E., Huang, H. J., & Ferris, D. P. (2015). Independent Component Analysis of Gait-Related Movement Artifact Recorded using EEG Electrodes during Treadmill Walking. *Front Hum Neurosci, 9*, 639. doi: 10.3389/fnhum.2015.00639

Springer, S., Giladi, N., Peretz, C., Yogev, G., Simon, E. S., & Hausdorff, J. M. (2006). Dual-tasking effects on gait variability: the role of aging, falls, and executive function. *Mov Disord, 21*(7), 950-957. doi: 10.1002/mds.20848

Thompson, J. D., & Franz, J. R. (2017). Do kinematic metrics of walking balance adapt to perturbed optical flow? *Hum Mov Sci, 54*, 34-40. doi: 10.1016/j.humov.2017.03.004

Tombu, M., & Jolicoeur, P. (2003). A central capacity sharing model of dual-task performance. *J Exp Psychol Hum Percept Perform, 29*(1), 3-18.

Varraine, E., Bonnard, M., & Pailhous, J. (2002). Interaction between different sensory cues in the control of human gait. *Exp Brain Res, 142*(3), 374-384. doi: 10.1007/s00221-001-0934-3

Vilhelmsen, K., van der Weel, F. R., & van der Meer, A. L. (2015). A high-density EEG study of differences between three high speeds of simulated forward motion from optic flow in adult participants. *Front Syst Neurosci, 9*, 146. doi: 10.3389/fnsys.2015.00146

Wagner, J., Makeig, S., Gola, M., Neuper, C., & Muller-Putz, G. (2016). Distinct beta Band Oscillatory Networks Subserving Motor and Cognitive Control during Gait Adaptation. *J Neurosci, 36*(7), 2212-2226. doi: 10.1523/JNEUROSCI.3543-15.2016

Wagner, J., Solis-Escalante, T., Grieshofer, P., Neuper, C., Muller-Putz, G., & Scherer, R. (2012). Level of participation in robotic-assisted treadmill walking modulates midline sensorimotor EEG rhythms in able-bodied subjects. *Neuroimage, 63*(3), 1203-1211. doi: 10.1016/j.neuroimage.2012.08.019

Walton, M. E., Croxson, P. L., Behrens, T. E., Kennerley, S. W., & Rushworth, M. F. (2007). Adaptive decision making and value in the anterior cingulate cortex. *Neuroimage, 36 Suppl 2*, T142-154. doi: 10.1016/j.neuroimage.2007.03.029

Warren, W. H., & Hannon, D. J. (1988). Direction of Self-Motion Is Perceived from Optical-Flow. *Nature, 336*(6195), 162-163. doi: Doi 10.1038/336162a0

Warren, W. H., Jr., Kay, B. A., Zosh, W. D., Duchon, A. P., & Sahuc, S. (2001). Optic flow is used to control human walking. *Nat Neurosci, 4*(2), 213-216. doi: 10.1038/84054

Winkler, I., Debener, S., Muller, K. R., & Tangermann, M. (2015). On the influence of high-pass filtering on ICA-based artifact reduction in EEG-ERP. *Conf Proc IEEE Eng Med Biol Soc, 2015*, 4101-4105. doi: 10.1109/EMBC.2015.7319296

Woollacott, M., & Shumway-Cook, A. (2002). Attention and the control of posture and gait: a review of an emerging area of research. *Gait Posture, 16*(1), 1-14.

Worden, M. S., Foxe, J. J., Wang, N., & Simpson, G. V. (2000). Anticipatory biasing of visuospatial attention indexed by retinotopically specific alpha-band electroencephalography increases over occipital cortex. *J Neurosci, 20*(6), RC63.

Yogev-Seligmann, G., Hausdorff, J. M., & Giladi, N. (2008). The role of executive function and attention in gait. *Mov Disord, 23*(3), 329-342; quiz 472. doi: 10.1002/mds.21720

Zeni, J. A., Jr., Richards, J. G., & Higginson, J. S. (2008). Two simple methods for determining gait events during treadmill and overground walking using kinematic data. *Gait Posture, 27*(4), 710-714. doi: 10.1016/j.gaitpost.2007.07.007